Marine Micropaleontology 137 (2017) 1–15

Contents lists available at ScienceDirect

Marine Micropaleontology

journal homepage: www.elsevier.com/locate/marmicro

Research paper

Inferred pseudo-cryptic speciation in the coccolithophore species *Braarudosphaera bigelowii* (Gran and Braarud) during the Early Paleocene (Danian)

Julia Criscione[a,*], David Bord[a,b], Linda Godfrey[a], Marie-Pierre Aubry[a]

[a] Department of Earth and Planetary Sciences, Rutgers University, 610 Taylor Road, Piscataway, NJ 08854-8066, USA
[b] ALS Oil & Gas, 6510 Guhn Road, Houston, TX 77040, USA

ARTICLE INFO

Keywords:
Braarudosphaera bigelowii
Lower/Middle Paleocene
Danian/Selandian boundary
Pseudo-cryptic speciation
Latest Danian event
Hyperthermal

ABSTRACT

Pseudo-cryptic speciation occurs commonly in living oceanic plankton. In the coccolithophores, recent genetic studies have revealed that *Braarudosphaera bigelowii* has a number of unique genotypes that correlate well with pentalith size, indicating that this coccolithophore "species" actually contains multiple pseudo-cryptic taxa. In order to look for evidence of pseudo-cryptic speciation in the past, we measured the radii of 2800 *B. bigelowii* pentaliths from the *Braarudosphaera*-rich limestones that contain the GSSP for the Lower/Middle Paleocene (Danian/Selandian) boundary at Zumaia, Spain. Analysis of the radius measurements using the Expectation-Maximization algorithm yielded two size groups, herein termed form X (< 4.5 μm) and form Y (≥ 4.5 μm). This result suggests the possibility of at least two pseudo-cryptic species in the Early Paleocene taxon *B. bigelowii*. In addition, there is a sharp increase in overall *B. bigelowii* abundance near the Paleocene Magnetochron C27n/26r reversal in the Zumaia section, forming an acme zone that spans approximately four meters. Isotopic analyses of organic matter show that an abrupt negative excursion of 3.5‰ in $\delta^{13}C_{org}$ coincided with the onset of the *B. bigelowii* acme. Biostratigraphic correlation between this section and the Danian/Selandian boundary section at Qreiya, Egypt confirmed that this isotopic shift correlates with a hyperthermal event (Latest Danian Event), and suggests that *B. bigelowii* abundance may have been affected by changing climatic conditions.

1. Introduction

As genetic analytical techniques continue to improve, reports of cryptic and pseudo-cryptic species are steadily increasing. Whereas cryptic species are morphologically identical, pseudo-cryptic species exhibit slight morphologic differences that allow their recognition independent of genetics (Amato, 2010). A number of recent molecular studies have shown that pseudo-cryptic speciation is common in coccolithophores (e.g., Geisen et al., 2002; Sáez et al., 2003; de Vargas et al., 2004; Sáez and Lozano, 2005; Hagino et al., 2009), as well as in other oceanic plankton (e.g., Amato and Montresor, 2008; Morard et al., 2009; Amato, 2010; Lundholm et al., 2012).

Braarudosphaera bigelowii is an extant coccolithophore species with a long geological record that extends back to the Lower Cretaceous (Berriasian Stage) (Perch-Nielsen, 1985; Bown et al., 1998; Burnett, 1998). Over its 100 million year (Myr) existence, this species has remained morphologically unchanged, with the exception of pentalith size (e.g., Stradner, 1960; Švábenická, 1999), which has ranged from ~1 μm (living cells, Hagino et al., 2009) to ~15.8 μm (Oligocene pentaliths, Steinmetz and Stradner, 1984) in radius. Takano et al. (2006), who first hypothesized pseudo-cryptic speciation in living *B. bigelowii*, also inferred pseudo-cryptic speciation in Turonian *B. bigelowii* based on the two size forms reported from the Bohemian Cretaceous Basin by Švábenická (1999). More recently, a genetic analysis of 15 living cells of *B. bigelowii* from the seas surrounding Japan revealed five distinct genotypes that correlate well with morphological differences in pentalith size (Takano et al., 2006; Hagino et al., 2009). It is possible that variations in pentalith size constitute evidence of pseudo-cryptic speciation through time.

The recent discovery of widespread pseudo-cryptic speciation among coccolithophore taxa has profound implications for the study of coccoliths preserved in sediments, as many of the morphologic (paleontologic) "species" are possibly suites of cryptic or pseudo-cryptic species. Sáez et al. (2003) and Geisen et al. (2004) alluded to the possibility of pseudo-cryptic speciation in the fossil record, but this phenomenon has not been formally considered as a mechanism for large morphological variations in extinct coccolithophores. Instead, these morphological differences are often interpreted as ecologic

* Corresponding author.
E-mail address: julicris@eps.rutgers.edu (J. Criscione).

http://dx.doi.org/10.1016/j.marmicro.2017.09.002
Received 27 October 2016; Received in revised form 1 September 2017; Accepted 10 September 2017
Available online 12 September 2017

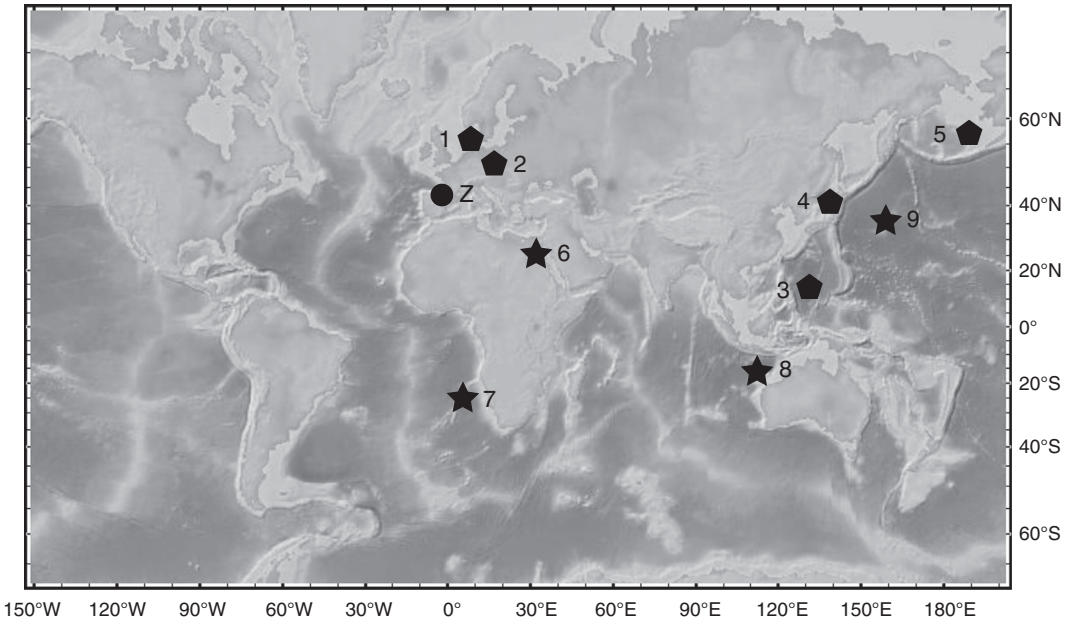

Fig. 1. Location map of areas discussed in text. Circle (Z): Zumaia. Pentagons: locations of *B. bigelowii* discussed herein, 1: Danish Basin (Clemmensen and Thomsen, 2005); 2: Bohemian Cretaceous Basin (Švábenická, 1999); 3: South China Sea (Fernando et al., 2013); 4: Seas around Japan (Takano et al., 2006; Hagino et al., 2009); 5: Bering Sea (Konno et al., 2007). Stars: locations of the LDE, 6: Qreiya, Egypt (Bornemann et al., 2009); 7: Walvis Ridge, ODP Leg 208 (Westerhold et al., 2011); 8: ODP Site 761B (Quillévéré et al., 2002); 9: Shatsky Rise, ODP Leg 198 (Westerhold et al., 2011). Map created using GeoMapApp.

responses (e.g., *Reticulofenestra* spp., Young, 1990; Beaufort, 1992). In this paper, we explore the possibility that the broad variations in size of *B. bigelowii* pentaliths during the Early Paleocene, as recorded in the Aitzgorri Limestone Formation (Basque Country, Spain), represent pseudo-cryptic speciation rather than intraspecific variability.

2. Materials and methods

2.1. The section: location, lithology, and age

The material studied here is from the limestones and marlstones in the vicinity of the GSSP (Global Boundary Stratotype Section and Point) for the Danian/Selandian boundary at Zumaia, Spain (Latitude: 43°17′57.1″ N, Longitude 2°15′39.6″ W; Fig. 1). We have examined a 17.1 m thick interval comprised of 13.9 m of *Braarudosphaera*-rich limestones with marly intercalations (Aitzgorri Limestone Formation), overlain by 3.2 m of mostly gray marlstones (Itzurun Formation). The Danian/Selandian boundary (astronomical age of 61.641 ± 0.040 Ma, Dinarès-Turell et al., 2010) corresponds to the formational contact between the upper Danian *Braarudosphaera*-rich limestones and the lower Selandian marlstones. These strata were deposited in the bathyal zone, at a water depth of approximately 1000 m (Pujalte et al., 1998; Bernaola et al., 2007). A summary of the lithology, sedimentology, and bathymetry of the section can be found in Schmitz et al. (2011).

The Zumaia section studied here spans Magnetochrons C27r (partim) to C26r (partim). The C27r/n and C27n/26r magnetic reversals are recorded near the base of the section (Dinarès-Turell et al., 2003), at 1.87 and 6.42 m, respectively. Based on calcareous nannofossil biostratigraphy (Schmitz et al., 2011), the section encompasses Zones NP4 and NP5 (Martini, 1971) and Zones NTp7a through NTp9 (Varol, 1989). It was deposited during the late Early and early Middle Paleocene and represents a duration of approximately 1.10 Myr based on Gradstein et al. (2012; see Appendix 1). Using the ages of the C27r/n and C27n/26r boundaries, we determined a sedimentation rate of ~1.54 cm/kyr for Magnetochronozone C27n, from which we extrapolated the ages of the samples, including the age of the bottom (~62.54 Ma) and the top (~61.44 Ma) of the section. We calculated an age of 61.58 Ma for the NP4/NP5 biozonal boundary, which differs by ~160 kyr from the age of ~59.95 Ma given by Agnini et al. (2014). This discrepancy may be due to a difference in the taxonomic concept of *Fasciculithus tympaniformis*, of which the lowest occurrence (LO) is sometimes difficult to locate. For instance, Agnini et al. (2007, p. 223) stated that there is some uncertainty in the precise placement of the LO of *F. tympaniformis* at ODP Site 1262 due to "the presence of transitional forms between *F. tympaniformis* and other fasciculith species." Likewise, Steurbaut and Sztrákos (2008) have shown that, contrary to general opinion, *F. tympaniformis* is not the first representative of the genus *Fasciculithus*. Therefore, its location at Zumaia may not be exactly correlative with its location at ODP Site 1262 (Agnini et al., 2007; Agnini et al., 2014), and we tentatively use an age of 61.44 Ma for the top of the Zumaia section (18.67 m).

2.2. Techniques and methods

Fifty-nine samples (Z1–Z59) of sedimentary rocks taken at intervals varying between 0.09 and 0.76 m are analyzed here (Fig. 2). These samples were collected by Dr. B. Schmitz for chronostratigraphic purposes (Schmitz et al., 2011) and they are the same as those studied by Bernaola et al. (2009). Forty-three of these samples are from the *Braarudosphaera*-rich limestones of the Aitzgorri Limestone Formation. The remaining sixteen samples are from the lower Itzurun Formation.

2.2.1. Micropaleontological analysis

All samples were prepared on standard smear slides, which were analyzed using a Zeiss Axioplan 2 Imaging microscope. We determined the relative abundance and preservation ratio (PR) of *Braarudosphaera bigelowii* within each sample by making a count along a single horizontal transect through the middle of each slide where material was most abundant. This ensured minimum bias due to sorting during the preparation of the smear slides. Relative abundance was established through semi-quantitative counts in a prefixed number of fields-of-view along the transect, and converting to the number of pentaliths per square millimeter (see methods in Backman and Shackleton, 1983). All pentaliths with at least two segments were counted, and the total number of two-segmented pentaliths was divided by two to prevent the "double-counting" of a single specimen. Single-segmented pentaliths

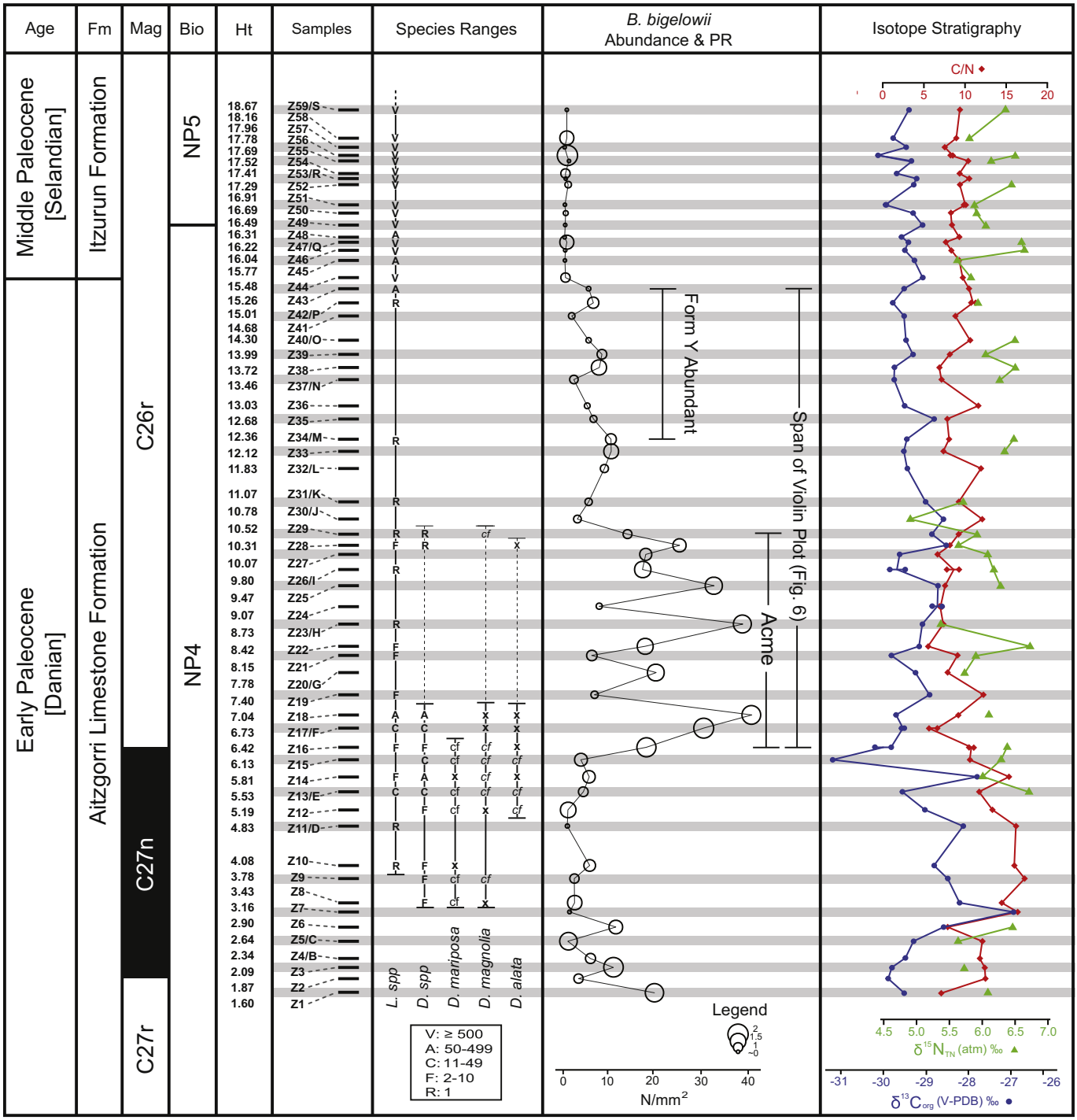

Fig. 2. Summary log of the Zumaia section including sample position, species ranges, *B. bigelowii* abundance & preservation ratio (PR), and isotope stratigraphy. Bars in the "Samples" column represent individual samples and are spaced according to their relative heights within the original section. Numbered sample IDs (i.e., Z1, Z2, etc.) are the same as those used in Bernaola et al. (2009); the letter IDs (i.e., B, C, etc.) were used in Bernaola (2002). The "Ht" column shows the heights used in this study, which were calculated from the lithologic column of Bernaola et al. (2009; their Fig. 3) using GraphClick software. The "Species Ranges" column shows the ranges of *Diantholitha* and *Lithoptychius* species. Their abundance in each sample is given as follows: V- Very abundant; A- Abundant; C - Common; F - Few; R - Rare (see legend). Total *Diantholitha* and *Lithoptychius* specimens were counted per slide. However, samples with very abundant *Lithoptychius* were quantified by extrapolating from the count per one vertical transect through the middle of the slide. For *Diantholitha* species, x indicates the presence of a species. If the specimen was very recrystallized and difficult to identify to species level, cf. is used instead. The "*B. bigelowii* Abundance and PR" column illustrates their abundance in number per square millimeter, and the PR of each sample by the size of the circle. A larger circle equates to a greater ratio of whole to broken pentaliths, while a smaller circle indicates a smaller ratio. The smallest circle approaches a ratio of 0 (see legend). Please note that N/mm^2 is a semi-quantitative metric (Backman and Shackleton, 1983), not a count of absolute abundance (N/g sediment; see also Andruleit, 1996). The "Isotope Stratigraphy" column gives C/N, $\delta^{13}C_{org}$ (V-PDB) ‰ and $\delta^{15}N_{TN}$ (V-PDB) ‰ values. Samples with two points were run twice. Samples with no $\delta^{15}N_{TN}$ value contained too little nitrogen to be detected. The position of the Danian/Selandian boundary follows Schmitz et al. (2011). The biozonation follows Martini (1971).

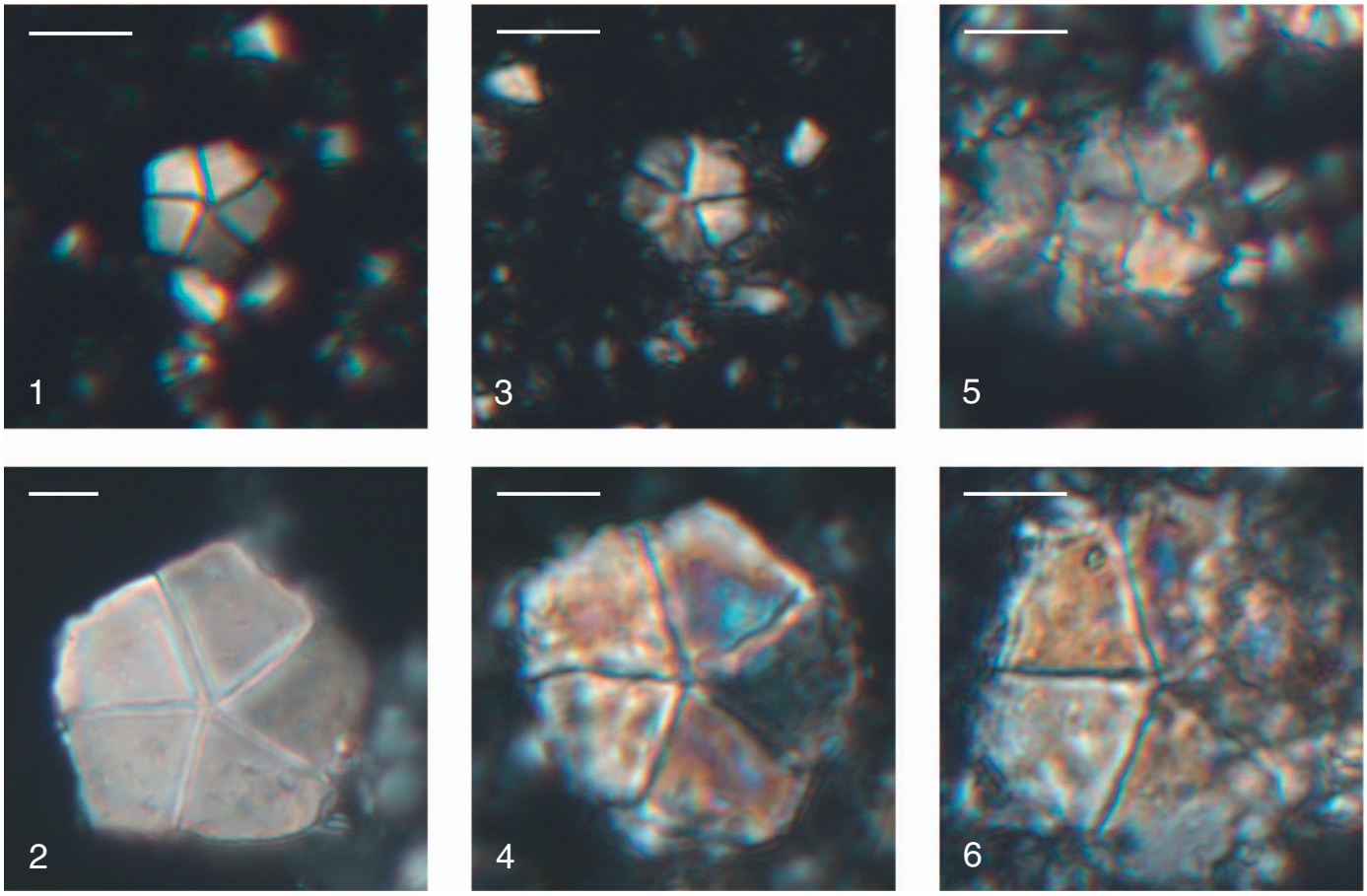

Plate 1. Range of preservation of *Braarudosphaera bigelowii* pentaliths. Preservation quality decreases from left to right. 1, 3, 5: form X; 2, 4, 6: form Y. Scale bars are 5 μm.

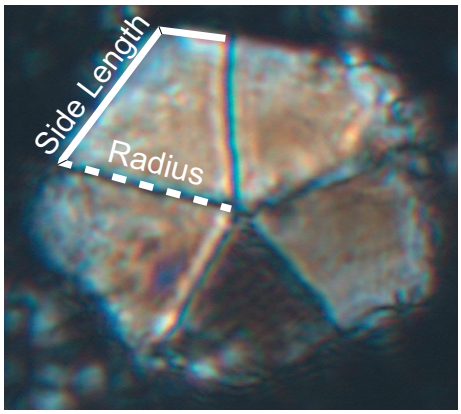

Fig. 3. Pentalith measurements were made on the least recrystallized segment per specimen. Radius was measured along the suture between adjacent segments (dashed line); side length was calculated by summing the short and long outer edges of the segment (solid lines).

were not included in the count because they would cause the "double-counting" of 2-, 3-, and 4-segmented pentaliths. Because determining preservation in regard to the state of recrystallization is subjective (Plate 1), we only took fragmentation into account. Therefore, the PR was estimated using the ratio of whole to broken pentaliths counted within the transect.

A semi-quantitative morphometric study was conducted on *Braarudosphaera bigelowii* pentaliths between 1.60 and 15.26 m (Z1 – Z43; an interval referred to as the "*Braarudosphaera* acme zone" by Bernaola et al., 2009). We focused on 6.42–15.26 m (Z16–Z43), the interval with the greatest abundance of pentaliths. One hundred pentaliths were photographed per sample in this interval, using an AxioCam HRc camera at 1600 × magnification, for a total of 2800 pentaliths. In order to compare our data with those of other authors (i.e., Hagino et al., 2009), the side length and radius of each photographed pentalith were measured using ImageJ software. The side length was measured by summing the lengths of the two outer edges of a single segment (Fig. 3). However, due to recrystallization, which first affected the corners and caused a rounding effect, the edges of the pentaliths tended to be irregular, causing uncertainty in the measurements. We remedied this problem by measuring the radius along the suture between adjacent segments. Because these two measurements have a linear relationship expressed by the equation $y = 0.7018x + 0.039$ (where x is side length and y is radius, $R^2 = 0.94$; shown in Supplementary Fig. 1), the radii can be compared to the side length measurements of other authors. Therefore, we chose to use the more reliable radius measurements throughout this study.

Model-based cluster analysis was performed in RStudio on the radii of all pentaliths using the Expectation-Maximization (EM) algorithm (mclust package; Fraley and Raftery, 2002; Fraley et al., 2012) in order to determine the presence of statistically significant size groupings.

In order to constrain the age of the *Braarudosphaera* acme, we conducted a biostratigraphic study of *Diantholitha* and *Lithoptychius* species (Plate 2), in which the total number of specimens was counted per slide. These taxa were chosen for study because they have proven useful for long distance correlation between upper Danian sediments (Aubry et al., 2011; Monechi et al., 2013).

2.2.2. Geochemical analysis

We conducted isotopic analysis of organic carbon ($\delta^{13}C_{org}$) and total

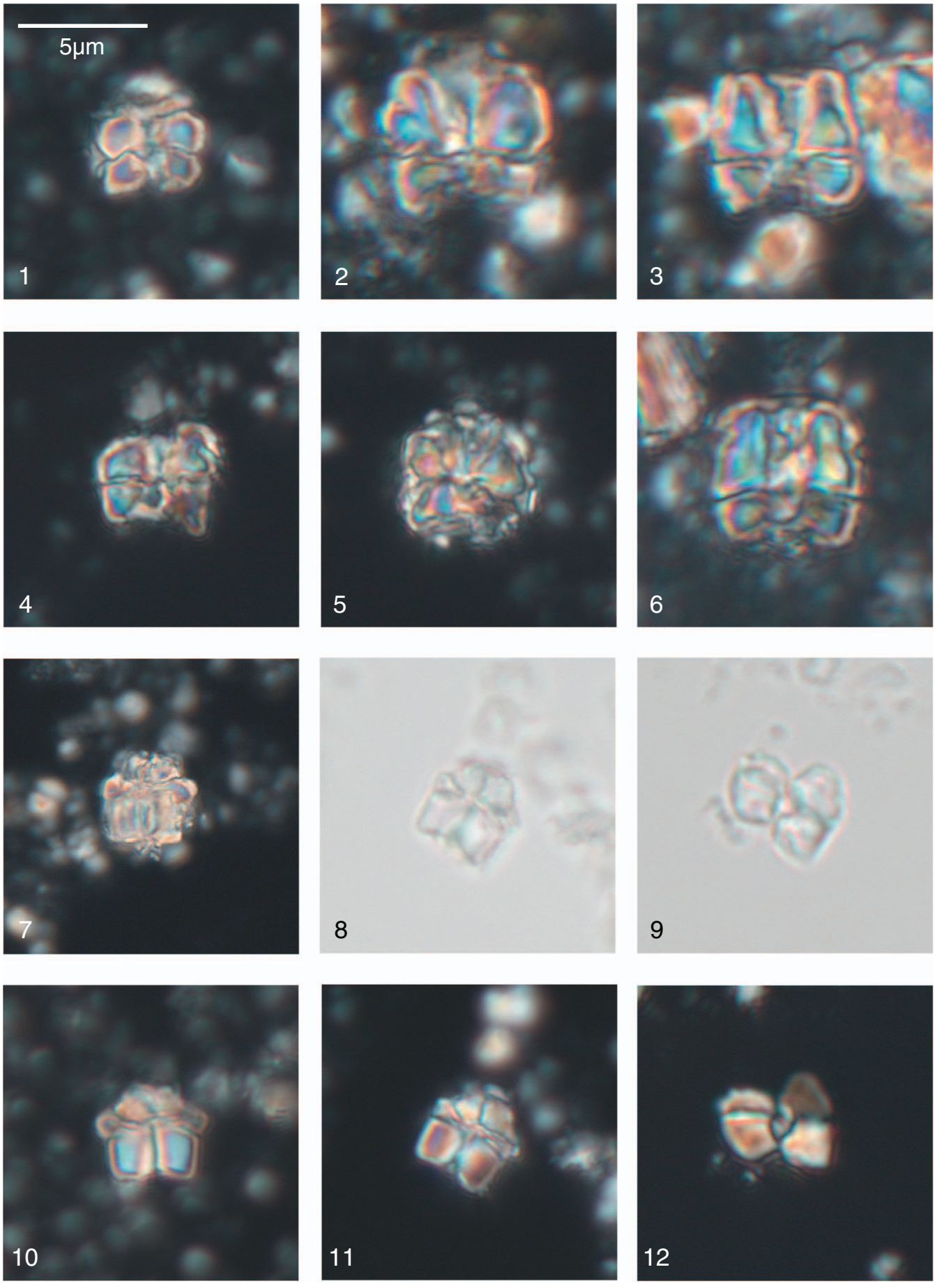

(caption on next page)

Plate 2. *Diantholitha* and *Lithoptychius* coccoliths. 1, 4: *Diantholitha* cf. *D. mariposa*, (1) sample Z16 (HO), (4) sample Z8 (LO); 2, 5: *D. magnolia*, (2) sample Z18 (HO), (5) sample Z8 (LO); 3, 6: *D. alata*, (3) sample Z18 (HO), (6) sample Z14; 7: *Lithoptychius* sp. cf. *L. collaris*, sample Z10 (LO of genus). 8, 10, 11: *L. collaris*, sample Z13; 9, 12: *L. varolii*, sample Z11. Scale bar for all specimens located in photo 1.

nitrogen ($\delta^{15}N_{TN}$), plus the carbon/nitrogen ratio (C/N) in an attempt to determine potential causes of variability in the abundance of *Braarudosphaera bigelowii* at Zumaia. Each sample was crushed into a powder using a mortar and pestle and carbonate was removed using 25% HCl. The residue was washed, dried, and weighed in a tin capsule. The analyses were performed at Rutgers University using a Eurovector Elemental Analyzer coupled with a GVI Isoprime100 CF-IRMS. The carbon isotope composition was normalized against NBS 22 (Coplen et al., 2006), isotopically characterized sorghum flour (Elementar), and an in-house secondary sediment standard. Organic carbon and total nitrogen concentrations were determined using the major ion peak areas and an acetanilide calibration line. Analysis of $\delta^{15}N_{TN}$ was also performed in a similar process using standards IAEA N-1 and IAEA N-3 (Qi et al., 2003). However, because some nitrogen can be bound within the carbonate lattice (e.g., Ren et al., 2009), $\delta^{15}N_{TN}$ was measured on bulk sediment with an ascarite trap to remove CO_2.

3. Results and discussion

3.1. Abundance and preservation of Braarudosphaera bigelowii pentaliths

Pentalith abundance is highly variable throughout the section and ranges from 0 pentaliths per square millimeter at 16.31 and 17.96 m (Z48 and Z57) to 42.9 pentaliths/mm^2 at 7.04 m (Z18) (Fig. 2). The average abundance throughout the section is 8.1 pentaliths/mm^2. At the base of the section (1.60 m; Z1), they are abundant, with 20.6/mm^2. This number then decreases to an average of 4.2/mm^2 between 1.87 and 6.13 m (Z2 and Z15). Between 6.42 and 10.52 m (Z16 and Z29), abundance oscillates from very few to > 40 pentaliths/mm^2, with an average of 21.9/mm^2. The *Braarudosphaera* acme zone, as defined in this work, corresponds to a duration of approximately 260 kyr (62.22 − 61.96 Ma; Appendix 1). Above it, abundance drops significantly. Between 10.78 and 15.26 m (Z30 and Z43), there are some intervals of greater abundance, but pentaliths do not exceed a density of 10.7/mm^2. Beginning at 15.48 m (Z44; Itzurun Formation), there are very few pentaliths present in each sample and their abundance decreases to ≤ 1 per mm^2.

The preservation ratio (PR), quantified as the ratio of whole to broken pentaliths per square millimeter, is variable throughout the section. The lower part of the section, 1.60 to 10.52 m (Z1 to Z29), contains a higher proportion of whole to broken pentaliths (average ratio of 1.4), while the upper part, 10.78 to 18.67 m, (Z30 to Z59), has a lower proportion of whole pentaliths (average ratio of 0.8). The PR tends to correlate well with abundance (Fig. 2). Samples with a greater abundance tend to have a higher PR, while samples with a low abundance tend to have a lower ratio. For example, 7.04 m (Z18) has 274 whole and 138 broken pentaliths, while 7.40 m (Z19) has 35 whole and 40 broken pentaliths. This could imply that low abundance is actually a result of increased fragmentation. If most of the pentaliths within a sample had been broken into isolated segments, they would not have been counted in this study, and abundance would appear lower. Thus, it is possible that the acme of *B. bigelowii* is stratigraphically more extensive and less variable than proposed here, perhaps explaining the larger acme zone described by Bernaola et al. (2009).

3.2. Pentalith measurements and comparisons

The Zumaia pentaliths vary broadly in size, with radii ranging from 1.4 to 10.6 μm. Plotting count against radius yields a bimodal distribution (Fig. 4) with the more prominent peak centered at ~3.0 μm and the smaller peak centered at ~6.5 μm. The EM method of model-based clustering (Fraley and Raftery, 2002; Fraley et al., 2012) was used to determine the number of statistically significant size groupings present within Zumaia *B. bigelowii*. This program uses Bayesian Information Criterion (BIC) values as a means for model selection, favoring the model with the largest value (Fraley and Raftery, 1999). The EM analysis yielded BIC values of − 10,362.900, − 8496.393, and − 8487.693 for one, two, and three groups, respectively. The three-group model had the largest BIC value, with cutoffs between the size groupings at 2.5 and 4.5 μm. However, its BIC value was very close to that of the two-group model, which had a cutoff value of 4.5 μm. Due to the continuous pentalith size variation and lack of clear morphological differences between groups, we cannot support the three-group model within the parameters of this study. Thus, we chose the two-group model with a cutoff value of 4.5 μm, which is also consistent with the bimodal distribution of pentalith radii. The smaller form, here termed form X, includes all specimens smaller than 4.5 μm in radius and constitutes approximately 82% of the assemblage. The larger form, here termed form Y, includes all specimens greater than or equal to 4.5 μm in radius and represents the remaining 18% of the assemblage.

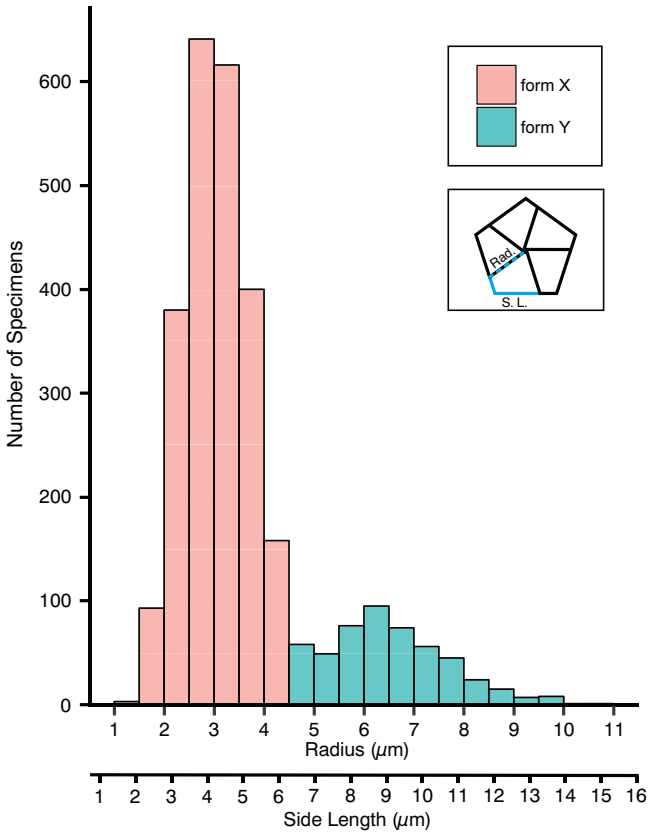

Fig. 4. Distribution of pentalith radii at Zumaia. The large peak represents form X; the smaller peak represents form Y. The cutoff value between the two forms is 4.5 μm based on the model-based cluster analysis performed with the mclust package in RStudio.

Both forms co-occur throughout the interval; form X is consistently abundant while form Y varies in abundance, as shown by the violin plot in Fig. 5. Form Y is less common between 6.42 and 11.83 m (Z16 and Z32), with an average of 11%, but its abundance its generally higher between 12.12 and 15.26 m (Z33 and Z43) with an average of 30%. However, the abundance of form Y in a few upper samples (e.g., 13.03, 14.68 m; Z36, Z41) is comparable to that in the lower part of the interval (12% and 11%, respectively). Meter 12.36 (Z34) has the greatest

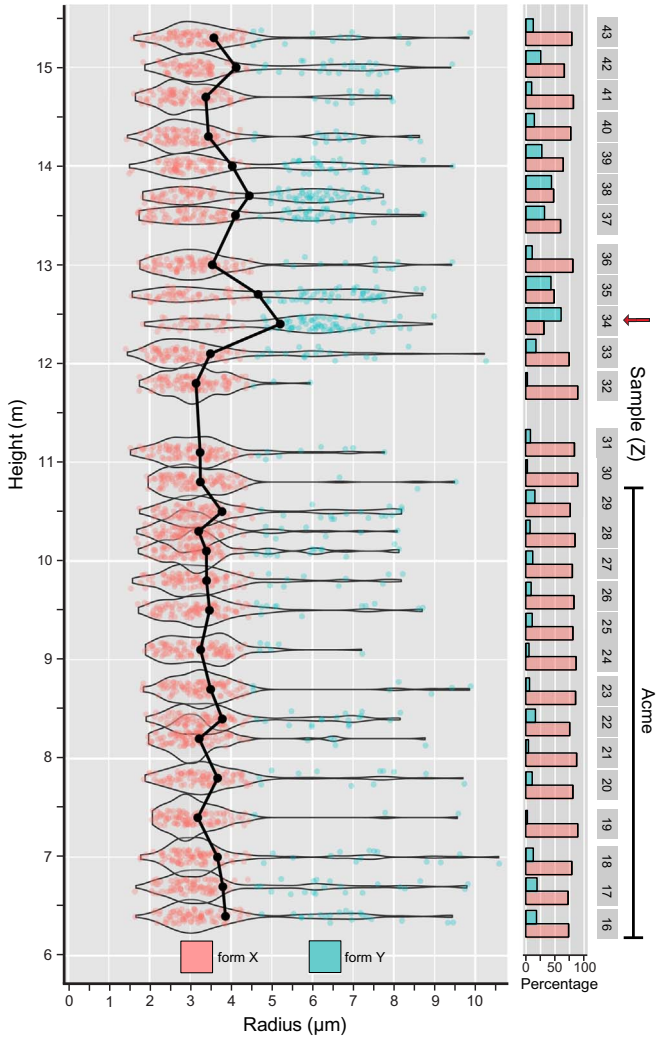

Fig. 5. Violin plot of pentalith radius versus height in the section. The vertical spread indicates the abundance of that radius measurement in the sample. Points are jittered to prevent overplotting. The black line represents the mean of each sample. Histograms show the percentages of forms X and Y in each sample. The sample with the arrow (Z34) is the only one that contains a greater proportion of form Y than form X.

percentage (66%) of form Y, while 7.40, 10.78 and 11.83 m (Z19, Z30 and Z32) have the smallest percentage (3% each). Meters 12.68 and 13.72 (Z35 and Z38) have about equal percentages of both forms (47% and 48% form Y, respectively). Only 12.36 m (Z34) has more specimens of form Y than form X (66% form Y).

In order to examine pentalith size variation through time, we compare the size of *B. bigelowii* pentaliths from the upper Lower Paleocene Aitzgorri Limestone Formation (this study), with those preserved in 1) Turonian deposits from Bohemia (Czech Republic; Švábenická, 1999), 2) Recent sediments from the South China Sea (Fernando et al., 2013) and 3) pentaliths in situ on coccospheres recovered from living plankton in the seas surrounding Japan (Takano et al., 2006; Hagino et al., 2009) and in the Bering Sea (Konno et al., 2007). The Early Paleocene pentaliths differ from the others in two significant aspects. First, they have a much wider range in size, and second, size variation is continuous, with no discrete groupings as reported in previous studies.

The Paleocene pentaliths at Zumaia consist of two size groups that range from 1.4 to 10.6 μm in radius (Fig. 6). The Turonian samples also contain two size groups (Švábenická, 1999), but their size range is much smaller than that of the Paleocene ones. While the number of specimens and methods of measurement were not described by Švábenická (1999), Takano et al. (2006) calculated their side lengths, which we, in turn, converted to radius. The "small form" ranges from 2.3 to 3.7 μm and overlaps with our form X. The Turonian "normal form" ranges from 5.5 to 6.4 μm and overlaps in size with the smaller end of the range of form Y.

The Paleocene pentaliths also differ from Recent (sub-fossil) and living pentaliths. The Recent pentaliths collected from surface sediments of the Western South China Sea by Fernando et al. (2013) compare well with the size groupings of pentaliths on living cells analyzed by Takano et al. (2006) and Hagino et al. (2009), as could be expected. Pentaliths on living cells ranged from 1 to 6.4 μm in radius (Takano et al., 2006; Konno et al., 2007; Hagino et al., 2009). Based on both size and genotype, Hagino et al. (2009, their Figure 3) distinguished four size classes and five pseudo-cryptic species within living *B. bigelowii* from the seas surrounding Japan: "small form" (< 1.7 μm in radius), "Intermediate form-A" (2.8–3.8 μm; includes Genotypes I and II), "Intermediate form-B" (3.8–5.1 μm; includes Genotype III) and "Large form" (> 5.3 μm; includes Genotypes IV and V). The smallest pentaliths on living cells are slightly smaller than the smallest pentaliths of Paleocene form X (1.0 μm versus 1.4 μm). However, the maximum size of Paleocene form Y is considerably larger than the largest pentaliths found on living *B. bigelowii* cells (10.6 μm versus 6.4 μm). Approximately 60% of the Zumaia pentaliths are of sizes recorded in living cells by Hagino et al. (2009; Table 1). The size range of form X overlaps with most of their "small form," all of "Intermediate form-A," and part of "Intermediate form-B," while form Y overlaps with part of "Intermediate form-B," all of their "Large form" and extends much beyond the upper size limit of the living cells. It is possible that the full size range of living *B. bigelowii* has not been sampled, whether in terms of intermediate or extreme values. In fact, both Konno et al. (2007) and Fernando et al. (2013) reported pentaliths with sizes in between those of the "small form" and "Intermediate form-A," which Fernando et al. (2013) termed "small form B." It is possible that "small form B" is actually a continuation of "Intermediate form-A" that was undetected in previous studies due to sampling location, scarcity, or other biological/ecological factors. However, with regard to the full amplitude of size difference, a survey of the literature has not revealed any reports of living *B. bigelowii* of a comparable size to (or larger than) the upper size range of form Y (Aubry, 2013).

When the size distributions of *B. bigelowii* from all four time intervals are compared, it is clear that the size of the Early Paleocene pentaliths differs markedly from those of the other samplings in both range and continuity (Fig. 6). The Paleocene pentaliths are the most varied in size, ranging from about as small as the smallest of the living to almost twice as large as the largest of the living. Despite these differences, the abundance patterns related to size are the same, with the larger forms always being less common. Hagino et al. (2009; their Fig. 3) reported only five specimens of the "Large form" making up 2.8% of their sample. Likewise, Fernando et al. (2013) found only a single specimen (1/303 or 0.3%) that corresponds to the "Large form." The Zumaia material also contains proportionally fewer large pentaliths than small ones, with a ratio of 426/2800 (~15%) equivalent to or larger than the "Large form" of Hagino et al. (2009). However, due to the differing size ranges of the "Large form" (living) and form Y (Paleocene), these two morphotypes may represent different genotypes and are more likely discrete products of pseudo-cryptic speciation.

Another difference concerning the distribution of pentalith size during the Early Paleocene and at Present (0 Ma; = living + Recent) must also be considered. The size distribution of pentaliths in Present *B. bigelowii* is discontinuous (Fig. 6). A relatively large gap in size between the small and intermediate forms (1.1 μm in Hagino et al., 2009; 0.8 μm in Fernando et al., 2013) occurs between Present small and intermediate forms. A slightly larger gap of 1.8 μm also occurs among the Turonian pentaliths, although between larger fractions. In contrast, the size distribution was continuous in the Paleocene, with no such gap. Two scenarios could account for the continuous size distribution of the

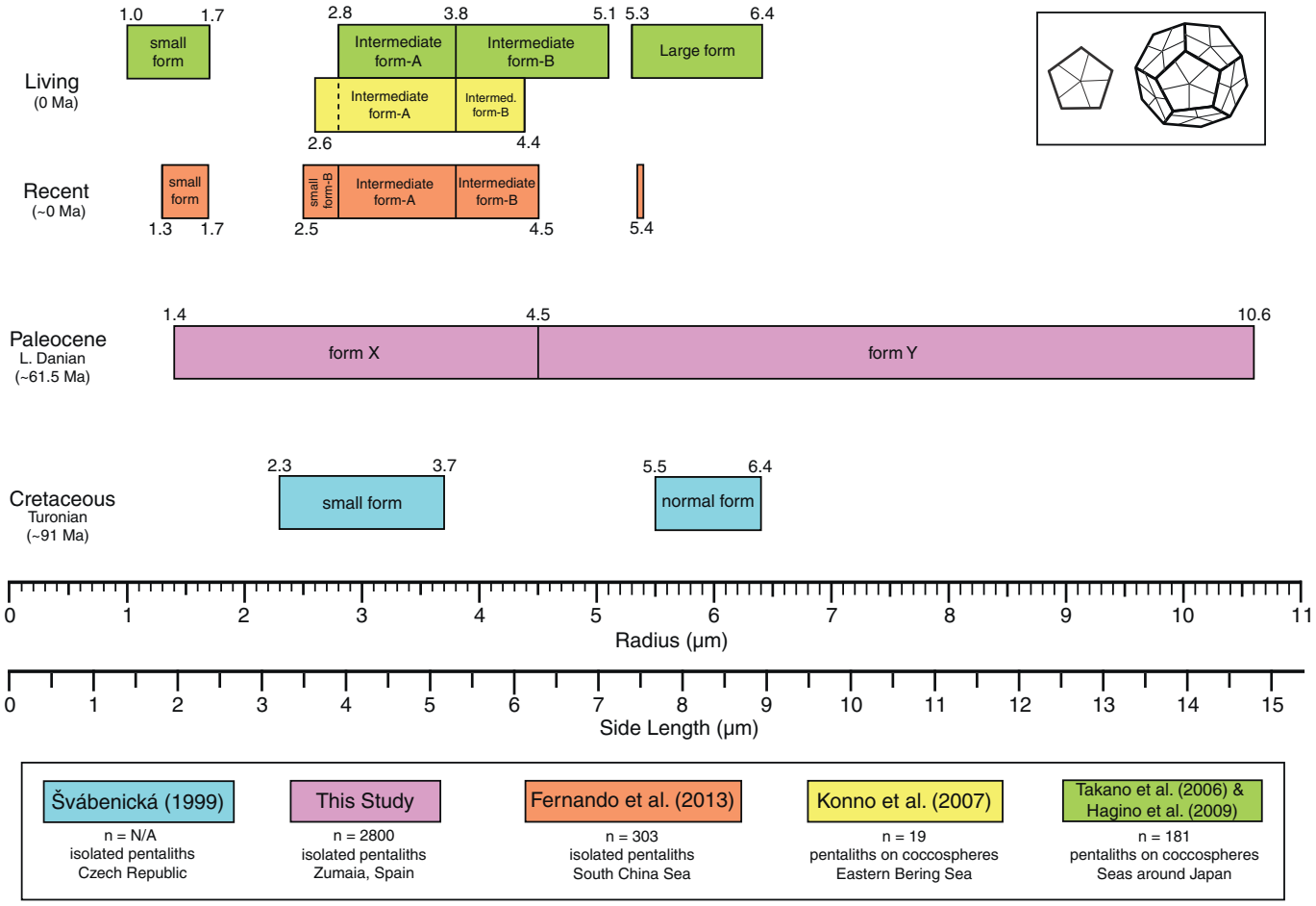

Fig. 6. Comparison of *B. bigelowii* radius measurements for the Living, Recent, late Danian, and Turonian. n is the number of specimens measured in each study. Names of size classes are homogenized after Hagino et al. (2009). Numbers located at size class boundaries are the radii measurements converted from original side lengths using the equation in Supplementary Fig. 1. The upper size limit (3.7 μm) of the Turonian small form was converted from the original side length value given by Takano et al. (2006), due to a discrepancy in its value later reported by Hagino et al. (2009).

Table 1
Comparison of the number of Zumaia pentaliths that correspond to each size class of Takano et al. (2006) and Hagino et al. (2009).

Size Class	Size Range (μm)	# at Zumaia	% at Zumaia
Small form	< 1.7	13/2800	0.5%
Intermediate form-A	2.8–3.8	1142/2800	41%
Intermediate form-B	3.8–5.1	359/2800	13%
Large form	> 5.3	171/2800	6%

Table 2
Comparison of the number of isolated pentaliths and pentaliths in situ on coccospheres measured in each study. Numbers in parentheses are the conversions; numbers without parentheses are the original numbers of pentaliths measured in each study.

	Number of pentaliths	Number of coccospheres
This study	2800	(233)–2800
Konno et al. (2007)	19	19
Takano et al. (2006) & Hagino et al. (2009)	181	181
Fernando et al. (2013)	303	(25)–303

Paleocene pentaliths. Because form Y is scarce in the lower part of our record but becomes more abundant in its upper part, it is possible that we are witnessing the beginning of the divergence of form Y from form X. Alternatively, the observed pattern may indicate changes in forcing of some ecological factor that selected for a broad range of sizes (morphotypes) in a single species.

In order to eliminate sampling bias as a cause for the difference in size distribution between Present and Paleocene pentaliths, we compare the number of pentaliths measured in each study (Table 2). A total of 2800 isolated Paleocene pentaliths were measured in this study. Konno et al. (2007) and Hagino et al. (2009) measured one pentalith on each of 19 and 181 living coccospheres, respectively. In addition, Fernando et al. (2013) measured 303 Recent isolated pentaliths. This is a total of 503 Present pentaliths.

Two assumptions can be made in order to compare Present and Paleocene pentaliths. On the one hand, it can be assumed that all of the measured isolated pentaliths are from different coccospheres. In this case, our sample size is much larger than that for the Present since the 503 measured Present specimens equate to approximately 18% of the 2800 Paleocene specimens. Therefore, the lesser size variability in the Present *B. bigelowii* could be affected by their comparatively smaller sample size. However, because large pentaliths are quite rare in Present *B. bigelowii*, it is unlikely that their current size range is as large as that of *B. bigelowii* from Zumaia. On the other hand, it can be assumed that the isolated pentaliths originated from the same coccospheres. Because each coccosphere is composed of 12 pentaliths, an equivalent of 233 Paleocene coccospheres (this study), and 25 Recent coccospheres (Fernando et al., 2013) would have been measured. In this case, our data of 233 Paleocene coccospheres would compare well with the data of the 225 Present coccospheres (19 from Konno et al., 2007, 181 from

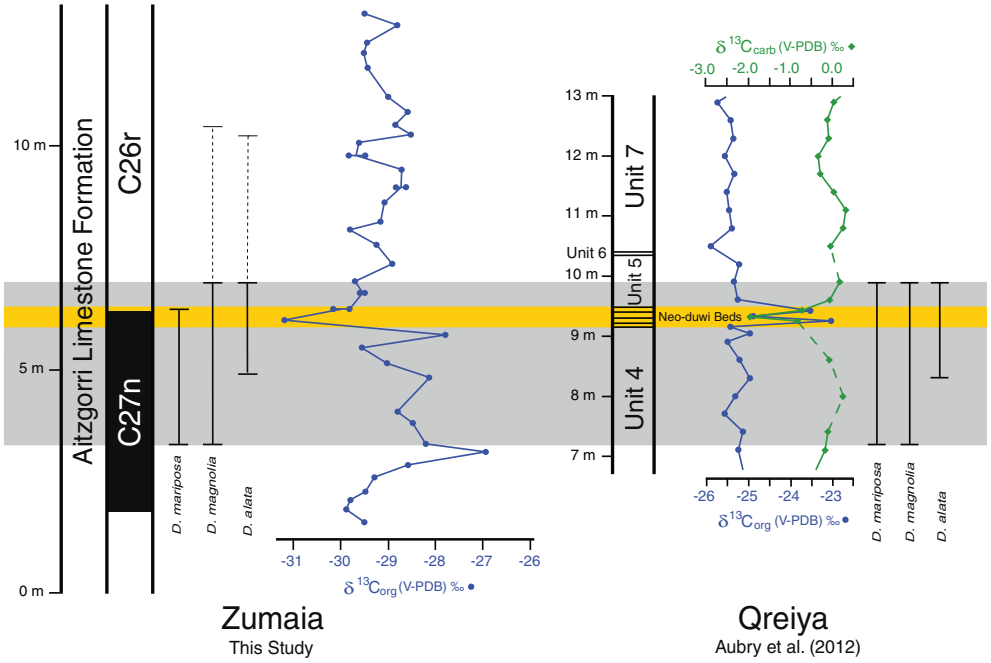

Fig. 7. Biostratigraphic correlation between the Zumaia and Qreiya sections. The gray band shows the range of *Diantholitha* spp. The yellow band highlights the Neo-duwi beds, in which the isotopic excursions occur at Qreiya. Isotope data and *Diantholitha* spp. ranges at Qreiya adapted from Aubry et al. (2012). Note that *D. magnolia* is referred to as *D. hemisphaerica* by this author. The complete carbon isotope record for Zumaia is illustrated in Bornemann et al. (2009, their Fig. 3). (For interpretation of the references to colour in this figure legend, the reader is referred to the web version of this article.)

Takano et al., 2006 & Hagino et al., 2009, and 25 from Fernando et al., 2013), and the sample size would not affect the data. However, it is more likely that the true number of measured coccospheres is somewhere in between these two estimates. Thus, the sample size of the Zumaia Paleocene pentaliths is probably somewhat larger than that for the Present, which could be a factor contributing to our size range that is both continuous and considerably larger.

In order to determine the full size range of *Braarudosphaera bigelowii* through time, we measured pentalith radii in photos of specimens published over time and compiled in a recent database (Aubry, 2013; Supplementary Fig. 2). Despite a lack of systematic investigations of *B. bigelowii* size, a few pentaliths as large and larger than those of Paleocene form Y have been documented throughout the Cenozoic. For instance, Early Eocene sediments of coastal Tanzania produced a pentalith ~9.2 μm in radius (Bown, 2005). Miocene deposits of West Africa, Austria, and Slovenia, have preserved a number of large pentaliths ranging from ~7.2–10.3 μm (Martini, 1969; Stradner and Fuchs, 1980; Bartol et al., 2008). Nishida (1971) documented a single large pentalith (8.3 μm) from the Early Pliocene of Japan, and Stradner (1973) recorded one of the same size from the early Quaternary of the Tyrrhenian Sea. A pentalith with an ~11.7 μm radius was illustrated from the Upper Paleocene-Lower Eocene of California (Bramlette and Sullivan, 1961), while the largest known pentalith would seem to be one with a radius of ~15.8 μm recorded from the Lower Oligocene of the eastern South Atlantic Ocean (Steinmetz and Stradner, 1984). From these data, the size difference between the largest known Cenozoic (Early Oligocene) pentalith and the largest pentalith from Zumaia is 5.2 μm, revealing that *B. bigelowii* had not yet reached its maximum size at the end of the Early Paleocene. Moreover, pentaliths more than twice as large as the largest measured on a living cell were secreted during the Early Oligocene. In fact, this extreme size difference between past and extant pentaliths had already been noted by Deflandre (1950), who observed that the diameter of a pentalith from the Lower Eocene of the Aquitaine Basin (France) was larger than the diameter of a living cell of *B. bigelowii*.

Conversely, small Cenozoic *B. bigelowii* pentaliths seem to be uncommonly reported in the literature (cf. Aubry, 2013; Supplementary Fig. 2), and very few are as small as the living ones reported by Hagino et al. (2009; 1.0 μm) and Fernando et al. (2013; 1.3 μm). As a reminder, the smallest pentaliths measured from Zumaia had a radius (measured along sutures) of 1.4 μm. Stradner (1960) first mentioned small pentaliths (< 10 μm in diameter) from the Miocene, and classified them as *B. bigelowii* subspecies *parvula* (though later authors did not use this name). Three small specimens were reported from Tanzania: Bown (2005) recorded a ~1.3 μm specimen from the Eocene and a ~1.6 μm specimen from the Late Paleocene, and Dunkley Jones et al. (2009) reported a ~2.2 μm specimen from the Late Eocene-Early Oligocene. Although there seems to be little or no record of very small pentaliths between the Early Oligocene and the Present, *B. bigelowii* pentaliths have rarely been documented from Neogene deposits.

Though we cannot assume that the full size range of *B. bigelowii* in today's plankton has been sampled, our current pentalith measurements and the review of size discussed above support the observation of Aubry (2007) of a long-term trend of decreasing size in coccolithophores through the Neogene. Pentaliths had begun to diversify in size as early as the Turonian, reaching their maximum size during the Oligocene. It would seem that during the Neogene, their size decreased and reached their minimum range in modern populations.

3.3. Species distribution within the Braarudosphaera acme zone

In order to establish potential causes of variability in *B. bigelowii* abundance at Zumaia, we determined the ranges of *Lithoptychius* and *Diantholitha* species (Fig. 2), which have been proposed to constitute good biostratigraphic markers in the vicinity of the Danian/Selandian boundary (see Aubry et al., 2012). Our objective in doing so was to date the *Braarudosphaera* acme zone. The first fasciculith assignable to *Lithoptychius* occurs at 4.08 m (Z10; Plate 2, Fig. 7), and is tentatively assigned to *L. collaris*. *Lithoptychius* fasciculiths occur fairly consistently above this level, but poor preservation hampers confident species identification. The first specimen reasonably assignable to *L. varolii* was recovered from 4.83 m (Z11; Plate 2, Figs. 9, 12). *Lithoptychius* spp. become very abundant at 15.48 m (Z44), while *Braarudosphaera* simultaneously become scarce. Coccoliths assignable to *Diantholitha* occur just below the acme at 3.43 m (Z8) and their highest occurrence (HO) at 7.04 m (Z18) is shortly above the onset of the acme of *B. bigelowii* (6.42 m; Z16). Two lone specimens of *Diantholitha* found at 10.31 and 10.52 m (Z28 and Z29) are considered reworked.

This study places the LO of the genus *Lithoptychius* (LO of *L. collaris*) approximately 1.5 m below that previously reported for Zumaia

(Monechi et al., 2013; LO at 5.53 meters, sample Z13). It also places the LO of *Diantholitha* spp. approximately 1.75 m below that reported by Monechi et al. (2013; LO at 5.19 meters; Z12). We attribute this discrepancy to a methodological difference in which we inventoried the entire smear slide, whereas Monechi et al. (2013, p. 30) state "only qualitative analyses were performed to accurately establish the succession of fasciculith bioevents." We note that Bown (2016, p. 29, Table 1) assigns *Diantholitha mariposa* and *Diantholitha*. spp. to Biozone NP5 and the Selandian Stage. This is based on the co-occurrence of multiple specimens of these taxa (as illustrated in op. cit., plate 8, Figs. 1–40) at the stratigraphic level labeled 7-1/46 in core TD site 27 (Tanzania) with "questionable specimens attributable to" and "that resemble" *Fasciculithus tympaniformis* (op. cit. p. 2 and 3), of which the LO defines the base of Zone NP5 (Martini, 1971). The specimen illustrated in plate 8, Fig. 3 from sample TD Site 27/7-1, 46 is not representative of *F. tympaniformis*. Taken collectively, *Diantholitha* species have a very narrow stratigraphic range associated with the late Danian radiation of the fasciculiths (Aubry et al., 2012). This range is restricted to a small interval in the upper part of Zone NP4 and to lowermost Chron C26r, whether at ODP Site 1262, Zumaia, or elsewhere (Aubry, 2015) and they constitute reliable stratigraphic markers to identify the late Danian hyperthermal event as we show below.

3.4. Geochemical analysis

We conducted isotopic analyses of organic carbon ($\delta^{13}C_{org}$), total nitrogen ($\delta^{15}N_{TN}$), and the carbon/nitrogen ratio (C/N) in an attempt to determine potential causes of variability in *B. bigelowii* abundance at Zumaia in relation to changes in the paleoenvironment. Pentalith abundance seems to show some correlation with the organic carbon record, but does not correlate well with the records of total nitrogen or the C/N ratio (Fig. 2). However, these two records do reveal information about the oceanic chemistry.

3.4.1. Total nitrogen

Total nitrogen ($\delta^{15}N_{TN}$) is often used as an indicator of paleoceanographic conditions. In nitrate-limited surface waters of the ocean, $\delta^{15}N_{TN}$ values closely match those of deep ocean nitrate that is mixed into the surface ocean (Tesdal et al., 2013). The $\delta^{15}N_{TN}$ of deep ocean nitrate during the Paleocene was approximately the same as that of today (L. G., unpublished data) with values of about 5‰ (Sigman et al., 2000). Though many samples had too little nitrogen for reliable $\delta^{15}N$ measurement, the $\delta^{15}N_{TN}$ values of Zumaia whole rock ranged from 4.9‰ at 10.78 m (Z30) to 6.7‰ at 8.42 m (Z22), with an average value of 6.1‰ (Fig. 2). Because these values are very close to those of deep ocean nitrate, this suggests that nitrate was quantitatively consumed and was therefore a limiting nutrient (Altabet and Deuser, 1985; Wada and Hattori, 1991). Thus, the nitrogen isotope values recorded at Zumaia suggest that the surrounding ocean was oligotrophic during the interval of Chrons C27r to C26r discussed here.

3.4.2. C/N ratio

The C/N ratio is a good proxy for determining the source of organic matter because it usually varies between 4 and 10 in phytoplankton-derived organic matter, whereas it is usually > 20 in land plants (Meyers, 1994). Additionally, this ratio has remained constant through time for a given source. The C/N ratio at Zumaia varies minimally throughout the section, ranging from 5.5 at 8.42 m (Z22) to 17.2 at 3.78 m (Z9), with an average value of 9.8 (Fig. 2). It has slightly elevated values (average of 15.1) between 3.16 and 5.81 m (Z7 and Z14), but is otherwise fairly stable. These higher values in the lower part of the section may indicate a mix of terrestrial- and marine-derived inputs. Around the Chron C27n/26r magnetic reversal, the C/N ratio decreases (average of 8.8), indicating that the organic matter source was marine. This could indicate less continental runoff (in agreement with oligotrophic conditions as indicated by total nitrogen) or water deepening (for which there is no information at this time).

3.4.3. Organic carbon isotopes

Organic carbon isotopes can be used, among other things, as a proxy for past productivity, levels of pCO_2, and to distinguish terrestrial and marine sources of organic carbon. Due to biological fractionation during photosynthesis, photosynthetic carbon has a negative $\delta^{13}C_{org}$ value relative to the carbon source (Hayes, 1993; Rau et al., 1996). This is applicable to marine and terrestrial organic carbon reservoirs, but terrestrial $\delta^{13}C$ ($\delta^{13}C_{TOM}$) is also dependent on other factors such as water availability. Today, terrestrial organic carbon is more depleted in ^{13}C than marine, but in the early Cenozoic, their $\delta^{13}C$ values were very similar, if not reversed (Strauss and Peters-Kotig, 2003; Falkowski et al., 2005).

The $\delta^{13}C_{org}$ record at Zumaia is highly variable in the lower part of the section but stabilizes in its upper part (Fig. 2). The values range from − 31.2 to − 26.9‰, with the minimum occurring at 6.13 m (Z15) and the maximum at 3.16 m (Z7). There is an increasing trend from 1.87 to 3.16 m (Z2 to Z7), followed by a 2.1 m interval with variable $\delta^{13}C_{org}$ values. Meters 6.42 to 18.67 (Z16 to Z59) are relatively stable between − 30.2 and − 28.5‰.

An important event in the section, however, is the negative shift of over 3‰ between 4.83 and 6.13 m (Z11 and Z15). The rather high $\delta^{13}C_{org}$ value at Z14 corresponds to an elevated C/N value, suggesting that this level contains higher terrestrial material and the signature is synchronous with the final stage of the negative $\delta^{13}C_{org}$ excursion which reaches its epitome at the Magnetochronozonal C27n/26r boundary. From the same section, Arenillas et al. (2008) reported an isotopic excursion of < 1‰ in carbonates (CIE-DS1, in their Fig. 3) spanning an interval of ~2.5 m, with the onset located about 1 m above the Magnetochronozonal C27n/26r boundary. Considering that both isotopic records are correlated to the same magnetostratigraphic record (Dinarès-Turell et al., 2003), straight correlation between isotope stratigraphy and magnetostratigraphy (Supplementary Fig. 3) would indicate that the $\delta^{13}C_{org}$ and $\delta^{13}C_{carb}$ record different isotopic excursions, one ($\delta^{13}C_{org}$) at the C27n/26r magnetic reversal, and the other ($\delta^{13}C_{carb}$) in early Magnetochron C26r. However, we note that the interval between the top of Magnetochronozone C27n and the formational contact between the Aitzgorri Limestone and the Itzurun reported by Arenillas et al. (2008) is ~12 m thick, while the thickness of the same interval in our study is ~9 m (as in Schmitz et al., 2011). We propose that this difference of three meters explains the discrepancy in the stratigraphic location of the two excursions, and consider that the excursion in $\delta^{13}C_{carb}$ reported by Arenillas et al. (2008) and the one in $\delta^{13}C_{org}$ documented here represent the same event.

Other authors have also reported negative $\delta^{13}C_{carb}$ events in the late Danian (around the C27n/26r magnetic reversal) from other sites. This includes the Latest Danian Event (LDE) at Qreiya, Egypt (Bornemann et al., 2009), the "Top Chron C27n Event" at ODP Legs 198 and 208 in the North Pacific and South Atlantic Oceans, respectively (Westerhold et al., 2008, 2011), and the $\delta^{13}C_{carb}$ excursion at ODP Site 761B offshore of Northwestern Australia (Quillévéré et al., 2002). Westerhold et al. (2011) suggested that all of these events, including CIE-DS1 (Arenillas et al., 2008) at Zumaia, represent a single, global, hyperthermal event. However, there has been some controversy concerning the LDE at Qreiya. Originally termed the "Neo-duwi event," (Guasti et al., 2005) it was first identified as a biotic excursion in which the foraminiferal species *Neoeponides duwi* moved into deeper waters following a change in sea level (Speijer, 2003). Bornemann et al. (2009) reported $\delta^{13}C_{carb}$ excursions of up to − 2‰ in the Neo-duwi event beds of three separate Egyptian sections, which they interpreted as evidence of the LDE at Qreiya. Subsequent isotopic analysis of the Neo-duwi beds also sampled at Qreiya found a negative $\delta^{13}C_{carb}$ excursion occurring simultaneously with a positive $\delta^{13}C_{org}$ excursion, which Aubry et al. (2012) interpreted as evidence of regional terrestrial input rather than a global hyperthermal event as suggested by Bornemann et al. (2009).

Using biostratigraphic correlation between the Zumaia and Qreiya sections, we are able to show that the $\delta^{13}C_{carb}$ excursion at Qreiya is correlative with the $\delta^{13}C_{org}$ excursion at Zumaia (Fig. 7). Due to overprinting of the magnetic signature of the Upper Paleocene-Lower Eocene succession at Qreiya (Kent and Dupuis, 2003), this section can only be correlated to the Zumaia section using biostratigraphy. The occurrence of the short-ranged species of *Diantholitha* in both sections allows us to determine the likely position of the Chron C27n/26r magnetic reversal at Qreiya, and consequently determine if the isotopic excursion within the Neo-duwi beds occurred simultaneously with the excursion at Zumaia. We correlate the *Diantholitha*-bearing interval between 3.43 and 7.04 m (Z8 and Z18) at Zumaia with the *Diantholitha*-bearing interval between 7.2 and 9.9 m at Qreiya (Aubry et al., 2011, 2012). At Zumaia, the LO of *Diantholitha* spp. occurs in lower Magnetochronozone C27n (3.43 m; Z8) and its HO in lowermost Magnetochronozone C26r (7.04 m; Z18). Since the C27n/26r magnetic reversal occurs in the uppermost part of the range of *Diantholitha* spp., we can predict the position of the magnetic reversal at Qreiya to also occur in the uppermost part of its range, at approximately 9.4 m (Aubry et al., 2012).

We can, in turn, correlate the positions of the isotopic excursions relative to the magnetochronology. The isotopic excursion at Zumaia occurred slightly before the magnetic reversal (latest Chron C27n; 6.13 m; Z15). By correlation, the excursion at Qreiya would have had to occur slightly below the magnetic reversal at 9.4 m, which it does, beginning approximately at 9.25 m. Thus, we conclude that the isotopic excursions at Zumaia and Qreiya were synchronous, and we reaffirm that the Neo-duwi event represents a local expression of the LDE at Qreiya. This allows us, in turn, to infer enhancement of the hydrological cycle (and associated increase in terrestrial input) during the LDE as a result of increased warmth, as initially shown by Schmitz and Pujalte (2003, 2007) for the Paleocene-Eocene Thermal Maximum (PETM). Neither the isotopes nor the C/N ratio measured at Qreiya by Aubry et al. (2012) provided clear evidence of a late Danian hyperthermal, unlike their joint signature in the deep-water (bathyal) section of Zumaia. Instead, the outer neritic section of Qreiya provided evidence of increased terrestrial input and runoff.

Based on this revision, the onset of the acme of *Braarudosphaera bigelowii* is correlated with the Danian/Selandian hyperthermal event, as shown by the steep negative shift in $\delta^{13}C_{org}$ between 5.81 and 6.13 m (Z14 and Z15) immediately preceding the onset of the acme (6.42 m; Z16). This suggests that the abundance of *B. bigelowii* was triggered by sudden climatic warming. However, one would assume that a hyperthermal-triggered acme event would terminate at the conclusion of the isotopic excursion. This is not what occurs at Zumaia; instead, the acme extends much beyond the end of the $\delta^{13}C_{org}$ excursion. This raises the question of whether there is a causal relationship between the two events: the close stratigraphic proximity of the isotopic excursion and the onset of the acme could be merely coincidental.

3.5. Evolutionary history

At Zumaia, form X was consistently abundant throughout late Chron C27n to early Chron C26r; form Y was also present throughout, but did not become abundant until ~61.84 Ma (early Chron C26r; Fig. 8). We propose three possible explanations for this pattern:

A. Forms X and Y diverged from a common ancestor (Fig. 8A). Both forms were present at Zumaia throughout the interval between 62.54 Ma and 61.44 Ma, but form Y became abundant at ~61.84 Ma, approximately 120 kyr after the acme of form X had ended.
B. Form Y diverged from form X at some time prior to the acme but its abundance was diluted by form X within this acme (Fig. 8B). This caused form Y to appear uncommon during Chron C27n and early Chron C26r. After the acme had ended, form Y became more abundant, giving the illusion of a speciation event at ~61.84 Ma.
C. A speciation event occurred at some time prior to the acme and the larger specimens found in the lower samples are the few remnants of a large form (form W) from that earlier speciation event (Fig. 8C). Form Y became abundant after a second speciation event (~61.84 Ma), where it diverged from form X. This would be evidence of iterative evolution.

Scenario A proposes that both forms X and Y diverged from a common ancestor. Because large pentaliths are already present by ~62.54 Ma, we cannot determine the ancestry of form Y. Therefore, we cannot exclude this possibility.

Scenario B proposes that the large pentaliths that occur throughout the acme are members of form Y. In this scenario, the abundance of form Y is diluted by the acme of form X, and form Y only becomes abundant at ~61.84 Ma, after the acme has ended (~120 kyr later), giving the illusion of a speciation event at this time. This scenario is plausible because the larger form is present in appreciable numbers both before and throughout the acme.

Scenario C, in which form Y is the result of a pseudo-cryptic speciation event at or slightly prior to 61.84 Ma, may be the most likely scenario. The larger specimens that lived before the speciation event at ~61.84 Ma would be the few remnants of an earlier speciation event (form W) due to their low abundance. In this scenario, the abundance of form X would have constituted a large genetic pool with increased genetic variability, allowing for the divergence of form Y slightly before the end of the acme. This new form Y would have proliferated after the acme of form X had ended (~120 kyr later), possibly due to the opening of a new ecological niche. This is an example of iterative morphologic evolution, a phenomenon that has been shown to occur in the plankton today (e.g., de Vargas et al., 2004). Recent genetic work on many groups of planktonic protists (including coccolithophores) suggests that in most cases, morphological "species" are actually suites of related "sibling species" (de Vargas et al., 2004). In a molecular phylogenetic study (Sáez et al., 2003), the sequencing of five coccolithophore morphospecies showed that each of them contained two or three distinct genotypes. Furthermore, there were no hybrids between the genetic types that inhabited the same areas, nor were there DNA mutations among geographically isolated individuals of the same genotype. Due to this lack of genetic exchange, it is apparent that these groups are reproductively isolated, and are therefore unique species (Sáez et al., 2003). De Vargas et al. (2004) proposed the term *super-species* to characterize these groups of morphologically similar but genetically differing species that evolve in geographic isolation.

This new understanding of coccolithophore super-species has profound implications for the study of coccoliths preserved in sediments, as many of the described "species" are likely super-species containing a number of cryptic species. Often, these species can be distinguished by slight morphological differences, making them "pseudo-cryptic species." The same scenario may be occurring with *B. bigelowii* at Zumaia, with the observed size variation resulting from pseudo-cryptic speciation (Fig. 9). In fact, the EM Analysis preferred the three group model with a BIC value marginally higher than that for two groups (−8487.693 and −8496.393, respectively). This may suggest that even form X represents more than one pseudo-cryptic species, though poor preservation precludes us from separating out additional species based on morphological characteristics. Moreover, the data from recent studies of living *B. bigelowii* show that this "species" is actually a super-species consisting of at least five genotypes (Hagino et al., 2009). Additionally, it is possible that the two size forms reported from the Turonian also represent super-species of *B. bigelowii*. Thus, it is probable that pseudo-cryptic speciation explains the size variability of *B. bigelowii* in the past.

Regardless of which scenario led to the proliferation of form Y at Zumaia, the sudden abundance of *B. bigelowii* would have increased the genetic pool, thereby increasing chances for genetic mutation. These

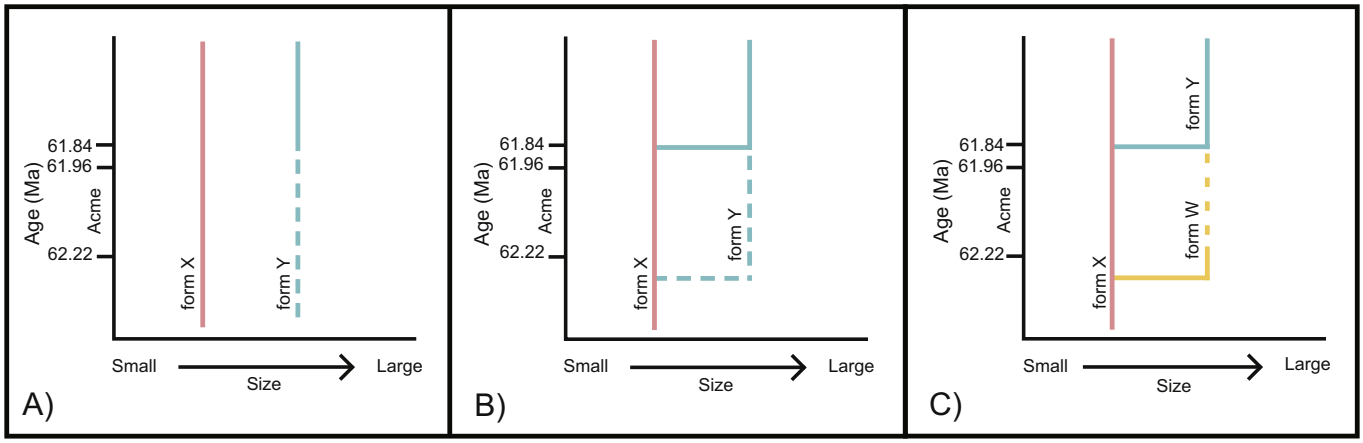

Fig. 8. Three proposed explanations for the abundance pattern of form Y. A) Forms X and Y evolved from a common ancestor. B) Form Y evolved before the acme and is present throughout the interval, but is diluted by the abundance of form X. Its sudden abundance at ~61.84 Ma gives the illusion of a speciation event at this level. C) The large pentaliths present in the lower part of the interval are remnants of an earlier speciation event; form Y evolved later (~61.84 Ma). Ages of samples are given in Appendix 1.

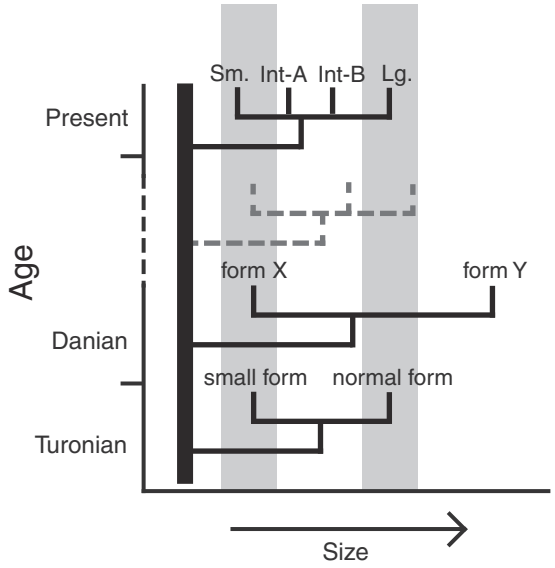

Fig. 9. Iterative morphologic evolution resulting in broad morphological species (= super-species) representing the repeated divergence of multiple cryptic species over time. Gray bands show similar *B. bigelowii* morphologies (small forms and large forms) repeatedly diverged from the main lineage over time.

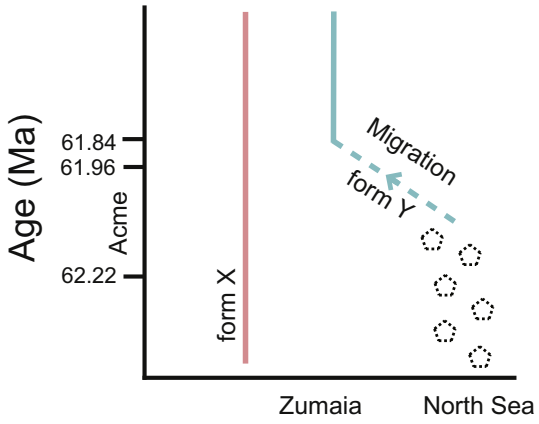

Fig. 10. Migration as an alternative hypothesis to explain the abundance of form Y. Form Y may have evolved in the North Sea during the acme of form X at Zumaia. It would have then migrated to Zumaia, giving the appearance of a speciation event at ~61.84 Ma. The sizes of late Danian pentaliths from the North Sea have not yet been reported.

mutations, in turn, could have allowed for greater environmental tolerances, and prompted phylogenetic divergence and pseudo-cryptic speciation. However, since the proliferation of form Y did not occur until ~61.84 Ma, approximately 400 kyr after the isotopic excursion, we see no evidence for a hyperthermal-induced divergence. Instead, its sudden abundance at ~61.84 Ma might have been caused by some other ecologic shift within the environment that allowed it to outcompete smaller form X. Such changes in environmental conditions (e.g., temperature, nutrient level) have been demonstrated to affect the dominance of different pseudo-cryptic species of living coccolithophores. Though on a much shorter timescale, the abundances of pseudo-cryptic species of *Calcidiscus leptoporus* have been shown to oscillate seasonally. *Calcidiscus leptoporus* subsp. *quadriperforatus* remains fairly constant throughout the year, while *C. leptoporus* subsp. *leptoporus* dominates the population during cool, mesotrophic conditions (Sáez et al., 2003). There is also a possibility that a similar scenario occurs in living and recent *B. bigelowii* populations. Hagino et al. (2009) reported only three "extraordinarily large" specimens (5.65, 5.72, and 6.36 μm in radius) around Japan, two from Furue Bay and one from the Yatsushiro Sea. In addition, Fernando et al. (2013) only reported one specimen (5.35 μm in radius) equivalent to the large form from a single site in the South China Sea (on the Sunda Shelf), far from the sites investigated in their study. In both instances, the larger cells inhabited areas different from most of the smaller ones, which may indicate differing environmental or chemical preferences between the pseudo-cryptic species of *B. bigelowii*. This idea of geographic separation leads to an alternative scenario to explain the sudden proliferation of form Y at Zumaia. It is possible that form Y evolved during the acme of form X, but in a different setting. *Braarudosphaera* was abundant in the North Atlantic and the North Sea Basin during the late Danian, and an acme zone occurs in the Danish Basin (Clemmensen and Thomsen, 2005; Bernaola et al., 2009). It is possible that form Y evolved in the North Sea and migrated to Zumaia (Fig. 10), which would give the illusion of its sudden divergence at ~61.84 Ma. It is also possible that form Y and the large form herein dubbed form W are sister pseudo-cryptic species. If so, several transient incursions occurred in the Zumaia area until the form finally became permanently established there. Future studies investigating the size of *B. bigelowii* in the North Sea and at intermediate sites between the Danish Basin and Zumaia, could determine if migration was, in fact, the mechanism by which form Y became abundant after ~61.84 Ma in the Zumaia section. Moreover, if it can be determined that the larger form Y exists elsewhere, this pseudo-cryptic species has the potential to become a useful biostratigraphic datum.

4. Conclusions

This study has examined the size variation in late Early Paleocene *Braarudosphaera bigelowii* from the vicinity of the GSSP for the Danian/Selandian boundary at Zumaia, Spain. The size distribution of the late Early and early Middle Paleocene *B. bigelowii* pentaliths differs distinctly from that of living specimens in both range and continuity, with a range almost twice that of the living specimens, and no discrete gaps in size. In addition, the Expectation-Maximization method of model-based cluster analysis yielded two size groupings based on pentalith radius: form X (< 4.5 μm) and form Y (≥ 4.5 μm). It is likely that these two forms are pseudo-cryptic species, though it is difficult to confirm this with morphologic analysis alone.

This study also reaffirms the presence of the LDE (Latest Danian Event) at Zumaia, and revealed a correlation between this hyperthermal event, as shown by the negative excursion in organic carbon isotopes, and the acme of *B. bigelowii*. While pentalith abundance increased dramatically at the onset of the hyperthermal, pentalith size was unaffected. It is therefore unlikely that the proliferation of form Y in the upper part of the section was climate-induced.

This is the first study to examine size in non-living, Cenozoic *Braarudosphaera bigelowii* and additional work is necessary to accurately reconstruct the evolutionary history of the taxon. We offer possible explanations for the abundance patterns observed in forms X and Y at Zumaia, but at this time, it is not possible to determine the true scenario. Though we cannot indisputably establish that forms X and Y are unique pseudo-cryptic species as genetic analysis is impossible, this study demonstrates the potential of morphometric analysis to assist in the documentation of pseudo-cryptic speciation in the past.

Responsibilities

This paper is an outgrowth of an Honors Thesis Project and represents a chapter of the Masters Thesis presented by JC towards an MSc at Rutgers University, under the supervision of MPA. All of the qualitative, quantitative (including abundance and size patterns), and comparative analyses of the coccolithophores were conducted by JC, who also determined the ages of the samples and correlated the Zumaia and Qreiya sections around the LDE. DB was responsible for the quantitative methodology, calculation of sample heights, and the statistical analysis of the *B. bigelowii* data. LG was responsible for the geochemical analysis.

Supplementary data to this article can be found online at http://dx.doi.org/10.1016/j.marmicro.2017.09.002.

Acknowledgements

Financial research support for this project came from a Graduate Teaching Assistantship from the Department of Earth and Planetary Sciences, Rutgers University. We would like to thank B. Schmitz for providing us with the samples upon which this study is based and whose biostratigraphic content was discussed at the *International Workshop of the Paleocene Working Group*, *Zumaia*, *Basque Country* in 2007, I. Arenillas for discussion on the stratigraphic position of their isotope record, W. A. Berggren for his thoughtful comments on the manuscript, and W. Si for discussion on the statistical analysis. We thank the two anonymous reviewers for their thoughtful comments that helped to improve this manuscript.

Appendix 1. Calculated ages for each Zumaia sample based on both Gradstein et al. (2012) and Cande and Kent (1995).

Sample	Height (m)	GTS2012 Age (Ma)	CK95 Age (Ma)
Z59	18.67	61.44	59.96
Z58	18.16	61.47	60.00
Z57	17.96	61.48	60.02
Z56	17.78	61.49	60.03
Z55	17.69	61.50	60.04
Z54	17.52	61.51	60.05
Z53	17.41	61.52	60.06
Z52	17.29	61.53	60.07
Z51	16.91	61.55	60.10
Z50	16.69	61.56	60.12
Z49	16.49	61.58	60.13
Z48	16.31	61.59	60.15
Z47	16.22	61.59	60.15
Z46	16.04	61.61	60.17
Z45	15.77	61.62	60.19
Z44	15.48	61.64	60.21
Z43	15.26	61.66	60.23
Z42	15.01	61.67	60.25
Z41	14.68	61.69	60.27
Z40	14.30	61.72	60.30
Z39	13.99	61.74	60.33
Z38	13.72	61.75	60.35
Z37	13.46	61.77	60.37
Z36	13.03	61.80	60.40
Z35	12.68	61.82	60.43
Z34	12.36	61.84	60.46
Z33	12.12	61.86	60.47
Z32	11.83	61.88	60.50
Z31	11.07	61.92	60.56
Z30	10.78	61.94	60.58

Z29	10.52	61.96	60.60
Z28	10.31	61.97	60.62
Z27	10.07	61.99	60.63
Z26	9.80	62.00	60.66
Z25	9.47	62.03	60.68
Z24	9.07	62.05	60.71
Z23	8.73	62.07	60.74
Z22	8.42	62.09	60.76
Z21	8.15	62.11	60.78
Z20	7.78	62.13	60.81
Z19	7.40	62.16	60.84
Z18	7.04	62.18	60.87
Z17	6.73	62.20	60.90
Z16	6.42	62.22	60.92
Z15	6.13	62.24	60.94
Z14	5.81	62.26	60.97
Z13	5.53	62.28	60.99
Z12	5.19	62.30	61.02
Z11	4.83	62.32	61.04
Z10	4.08	62.37	61.10
Z9	3.78	62.39	61.13
Z8	3.43	62.42	61.15
Z7	3.16	62.43	61.18
Z6	2.90	62.45	61.20
Z5	2.64	62.47	61.22
Z4	2.34	62.49	61.24
Z3	2.09	62.50	61.26
Z2	1.87	62.52	61.28
Z1	1.60	62.54	61.30

References

Agnini, C., Fornaciari, E., Raffi, I., Rio, D., Röhl, U., Westerhold, T., 2007. High-resolution nannofossil biochronology of middle Paleocene to early Eocene at ODP site 1262: Implications for calcareous nannoplankton evolution. Mar. Micropaleontol. 64 (3), 215–248.

Agnini, C., Fornaciari, E., Raffi, I., Catanzariti, R., Pälike, H., Backman, J., Rio, D., 2014. Biozonation and biochronology of Paleogene calcareous nannofossils from low and middle latitudes. Newsl. Stratigr. 47 (2), 131–181.

Altabet, M.A., Deuser, W.G., 1985. Seasonal variations in natural abundance of ^{15}N in particles sinking to the deep Sargasso Sea. Nature 315, 218–219.

Amato, A., 2010. Species concepts and definitions: reproductive isolation as a tool to reveal species boundaries. Int. J. Plant Reprod. Biol. 2 (2), 114–126.

Amato, A., Montresor, M., 2008. Morphology, phylogeny, and sexual cycle of *Pseudonitzschia mannii* sp. nov. (Bacillariophyceae): a pseudo-cryptic species within the *P. pseudodelicatissima* complex. Phycologia 47, 487–497.

Andruleit, H., 1996. A filtration technique for quantitative studies of coccoliths. Micropaleontology 42, 403–406.

Arenillas, I., Molina, E., Ortiz, S., Schmitz, B., 2008. Foraminiferal and $\delta^{13}C$ isotopic event-stratigraphy across the Danian–Selandian transition at Zumaya (northern Spain): chronostratigraphic implications. Terra Nova 20 (1), 38–44.

Aubry, M.-P., 2007. A major Pliocene coccolithophore turnover: change in morphological strategy in the photic zone. In: Monechi, S., Coccioni, R., Rampino, M. (Eds.), Large Ecosystem Perturbations: Causes and Consequences. Geological Society of America Special Paper 424. pp. 25–51.

Aubry, M.-P., 2013. Cenozoic Coccolithophores: Braarudosphaerales. Atlas of Micropaleontology series Micropaleontology Press, New York (336 pp).

Aubry, M.-P., 2015. Cenozoic Coccolithophores: Discoasteraerales. Atlas of Micropaleontology series Micropaleontology Press, New York (328 pp).

Aubry, M.-P., Bord, D., Rodriguez, O., 2011. New taxa of the order Discoasterales hay 1977. Micropaleontology 57, 269–287.

Aubry, M.-P., Rodriguez, O., Bord, D., Godfrey, L., Schmitz, B., Knox, R.W.B., 2012. The first radiation of the Fasciculiths: morphologic adaptations of the coccolithophores to oligotrophy. Aust. J. Earth Sci. 105 (1), 29–38.

Backman, J., Shackleton, N.J., 1983. Quantitative biochronology of Pliocene and Pleistocene calcareous nannofossils from the Atlantic, Indian and Pacific ocean. Mar. Micropaleontol. 8, 141–170.

Bartol, M., Pavsic, J., Dobnikar, M., Bernasconi, S.M., 2008. Unusual *Braarudosphaera bigelowii* and *Micrantholithus vesper* enrichment in the Early Miocene sediments from the Slovenian corridor, a seaway linking the central Paratethys and the Mediterranean. Palaeogeogr. Palaeoclimatol. Palaeoecol. 267, 77–88.

Beaufort, L., 1992. Size variations in late Miocene *Reticulofenestra* and implication for paleoclimatic interpretation. Sci. Geol. Mem. 43, 339–350.

Bernaola, G., 2002. Los nannofósiles calcáreos del Paleoceno en el dominio Pirenaico. In: Bioestratigraía, cronoestratigraía y paleoecología: Leioa. Doctoral thesis. University of the Basque Country (445 pp).

Bernaola, G., Baceta, J.I., Orue-Etxebarria, X., Alegret, L., Martín-Rubio, M., Arostegui, J., Dinarès-Turell, J., 2007. Evidence of an abrupt environmental disruption during the mid-Paleocene biotic event (Zumaia section, western Pyrenees). Geol. Soc. Am. Bull. 119 (7–8), 785–795.

Bernaola, G., Martin-Rubio, M., Baceta, J.J., 2009. New high resolution calcareous nannofossil analysis across the Danian/Selandian transition at the Zumaya section: Comparison with south Tethys and Danish sections. Geol. Acta 7, 79–92.

Bornemann, A., Schulte, P., Sprong, J., Steurbaut, E., Youssef, M., Speijer, R.P., 2009. Latest Danian carbon isotope anomaly and associated environmental change in the southern Tethys (Nile Basin, Egypt). J. Geol. Soc. 166 (6), 1135–1142.

Bown, P.R., 2005. Palaeogene calcareous nannofossils from the Kilwa and Lindi areas of coastal Tanzania (Tanzania Drilling Project 2003–4). Journal of Nannoplankton Research 27, 21–95.

Bown, P.R., 2016. Paleocene calcareous nannofossils from Tanzania (TDP sites 19, 27 and 38). Journal of Nannoplankton Research 36, 1–32.

Bown, P.R., Rutledge, D.C., Crux, J.A., Gallagher, L.T., 1998. Lower Cretaceous. In: Bown, P.R. (Ed.), Calcareous Nannofossil Biostratigraphy. Kluver Academic Publishers, London, pp. 86–131.

Bramlette, M.N., Sullivan, F.R., 1961. Coccolithophorids and related nannoplankton of the Early Tertiary in California. Micropaleontology 7, 129–174.

Burnett, J.A., with contributions from Gallagher, L. T., and Hampton, M. J, 1998. Upper Cretaceous. In: Bown, P.R. (Ed.), Calcareous Nannofossil Biostratigraphy. Kluver Academic Publishers, London, pp. 132–199.

Cande, S.C., Kent, D.V., 1995. Revised calibration of the geomagnetic polarity timescale for the Late Cretaceous and Cenozoic. J. Geophys. Res. Solid Earth 100, 6093–6095.

Clemmensen, A., Thomsen, E., 2005. Palaeoenvironmental changes across the Danian–Selandian boundary in the North Sea Basin. Palaeogeogr. Palaeoclimatol. Palaeoecol. 219 (3), 351–394.

Coplen, T.B., Brand, W.A., Gehre, M., Gröning, M., Meijerm, H.A.J., Toman, B., Verkouteren, R.M., 2006. New guidelines for $\delta^{13}C$ measurements. Anal. Chem. 78, 2439–2441.

Deflandre, G., 1950. Observations sur les Coccolithophoridés, à propos d'un nouveau type de *Braarudosphaeridé*, *Micrantholithus*, à éléments clastiques. In: Comptes Rendus (Hebdomadaires des Séances) de l'Académie des Sciences Paris. 231. pp. 1156–1158.

Dinarès-Turell, J., Baceta, J.I., Pujalte, V., Orue-Etxebarria, X., Bernaola, G., Lorito, S., 2003. Untangling the Palaeocene climatic rhythm: an astronomically calibrated Early Palaeocene magnetostratigraphy and biostratigraphy at Zumaia (Basque basin, northern Spain). Earth Planet. Sci. Lett. 216, 483–500.

Dinarès-Turell, J., Stoykova, K., Baceta, J.I., Ivanov, M., Pujalte, V., 2010. High-resolution intra-and interbasinal correlation of the Danian-Selandian transition (Early Paleocene): the Bjala section (Bulgaria) and the Selandian GSSP at Zumaia (Spain).

Palaeogeogr. Palaeoclimatol. Palaeoecol. 297 (2), 511–533.
Dunkley Jones, T., Bown, P.R., Pearson, P.N., 2009. Exceptionally well preserved upper Eocene to lower Oligocene calcareous nannofossils (Prymnesiophyceae) from the Pande Formation (Kilwa Group), Tanzania. J. Syst. Palaeontol. 7, 359–411.
Falkowski, P.G., Katz, M.E., Milligan, A.J., Fennel, K., Cramer, B.S., Aubry, M.P., Berner, R.A., Novacek, M.J., Zapol, W.M., 2005. The rise of oxygen over the past 205 million years and the evolution of large placental mammals. Science 309, 2202–2204.
Fernando, A.G.S., Fernandez, A.R.C., Wiesner, M.G., 2013. *Braarudosphaera bigelowii* morphotypes in the surface sediments of the southwestern South China Sea. Micropaleontology 59 (6), 579–586.
Fraley, C., Raftery, A.E., 1999. MCLUST: Software for model-based cluster analysis. J. Classif. 16, 297–306.
Fraley, C., Raftery, A.E., 2002. Model-based clustering, discriminant analysis and density estimation. J. Am. Stat. Assoc. 97, 611–631.
Fraley, C., Raftery, A.E., Murphy, T.B., Scrucca, L., 2012. mclust Version 4 for R: Normal Mixture Modeling For Model-Based Clustering, Classification, And Density Estimation, Technical Report No. 597. Department of Statistics, University of Washington (57 pp).
Geisen, M., Billard, C., Broerse, A., Cros, L., Probert, I., Young, J., 2002. Life-cycle associations involving pairs of holococcolithophorid species: intraspecific variation or cryptic speciation? Eur. J. Phycol. 37 (4), 531–550.
Geisen, M., Young, J.R., Probert, I., Sáez, A.G., Baumann, K.H., Sprengel, C., Bollmann, J., Cros, L., de Vargas, C., Medlin, L.K., 2004. Species level variation in coccolithophores. In: Thierstein, H.R., Young, J.R. (Eds.), Coccolithophores: From Molecular Processes to Global Impact. Springer Verlag, pp. 313–352.
Gradstein, F.M., Ogg, J.G., Schmitz, M., Ogg, G. (Eds.), 2012. The Geologic Time Scale 2012. Vol. 2 Elsevier Set. (1176 pp).
Guasti, E., Speijer, T.P., Fornaciari, E., Schmitz, B., Kroon, D., Gharaibeh, A., 2005. Transient biotic change within the Danian–Selandian transition in Egypt and Jordan. In: Guasti, E. (Ed.), Early Paleogene Environmental Turnover in the Southern Tethys as Recorded by Foraminiferal and Organic-walled Dinoflagellate Cysts Assemblages. Fachbereich Geowissenschaften der Universität Bremeb. Berichte, Bremen, pp. 75–110 (PhD Dissertation).
Hagino, K., Takano, Y., Horiguchi, T., 2009. Pseudo-cryptic speciation in *Braarudosphaera bigelowii* (Gran and Braarud) Deflandre. Mar. Micropaleontol. 72, 210–221.
Hayes, J.M., 1993. Factors controlling ^{13}C contents of sedimentary organic compounds: principles and evidence. Mar. Geol. 113 (1), 111–125.
Kent, D.V., Dupuis, C., 2003. Paleomagnetic study of the Paleocene-Eocene Tarawan chalk and Esna Shale: dual polarity remagnetizations of Cenozoic sediments in the Nile Valley (Egypt). Micropaleontology 49 (Suppl. 1), 139–146.
Konno, S., Harada, N., Narita, H., Jordan, R.W., 2007. Living *Braarudosphaera bigelowii* (Gran & Braarud) Deflandre in the Bering Sea. J. Nannoplankton Res. 29 (2), 78–87.
Lundholm, N., Bates, S.S., Baugh, K.A., Bill, B.D., Connell, L.B., Léger, C., Trainer, V.L., 2012. Cryptic and pseudo-cryptic diversity in diatoms- with descriptions of *Pseudonitzschia hasleana* sp. nov. and *P. fryxelliana* sp. nov. J. Phycol. 48, 436–454.
Martini, E., 1969. Nanoplankton aus dem Miozän von Gabon (Westafrika). Neues Jahrb. Geol. Palaontol. Abh. 132, 285–300.
Martini, E., 1971. Standard Tertiary and Quaternary calcareous nannoplankton zonation. In: Farinacci, A. (Ed.), Proceedings of the Second Planktonic Conference, Rome, (1970). 2. Edizioni Tecnoscienza, pp. 739–785.
Meyers, P.A., 1994. Preservation of elemental and isotopic source identification of sedimentary organic matter. Chem. Geol. 114 (3–4), 289–302.
Monechi, S., Reale, V., Bernaola, G., Balestra, B., 2013. The Danian/Selandian boundary at site 1262 (South Atlantic) and in the Tethyan region: biomagnetostratigraphy, evolutionary trends in fasciculiths and environmental effects of the latest Danian event. Mar. Micropaleontol. 98, 28–40.
Morard, R., Quillévéré, F., Escarguel, G., Ujiie, Y., de Garidel-Thoron, T., Norris, R.D., de Vargas, C., 2009. Morphological recognition of cryptic species in the planktonic foraminifer *Orbulina universa*. Mar. Micropaleontol. 71 (3), 148–165.
Nishida, S., 1971. Nannofossils from Japan IV. Calcareous nannoplankton fossils from the Tônohama Group, Shikoku, southeast Japan. In: Transactions and Proceedings of the Palaeontological Society of Japan, New Series. 83. pp. 143–161.
Perch-Nielsen, K., 1985. Mesozoic calcareous nannofossils. In: Bolli, H.M., Saunders, J.B., Perch-Nielsen, K. (Eds.), Plankton Stratigraphy. Cambridge University Press, Cambridge, pp. 329–426.
Pujalte, V., Baceta, J.I., Orue-Etxebarria, X., Payros, A., 1998. Paleocene strata of the Basque Country, western Pyrenees, northern Spain: facies and sequence development in a deep-water starved basin. In: Graciansky, P.C., Hardenbol, J., Jacquin, T., Vail, P.R. (Eds.), Mesozoic and Cenozoic Sequence Stratigraphy of European Basins. Society of Economic Paleontologists and Mineralogists Special Publication 60. pp. 311–325.
Qi, H., Coplen, T.B., Geilmann, H., Brand, W.A., Böhlke, J.K., 2003. Two new organic reference materials for $\delta^{13}C$ and $\delta^{15}N$ measurements and a new value for the $\delta^{13}C$ of NBS 22 oil. Rapid Commun. Mass Spectrom. 17 (22), 2483–2487.
Quillévéré, F., Aubry, M.-P., Norris, R.D., Berggren, W.A., 2002. Paleocene oceanography of the eastern subtropical Indian Ocean: an integrated magnetobiostratigraphic and stable isotope study of ODP Hole 761B (Wombat Plateau). Palaeogeogr. Palaeoclimatol. Palaeoecol. 184 (3), 371–405.
Rau, G.H., Riebesell, U., Wolf-Gladrow, D., 1996. A model of photosynthetic ^{13}C fractionation by marine phytoplankton based on diffusive molecular CO_2 uptake. Mar. Ecol. Prog. Ser. 133, 275–285.
Ren, H., Sigman, D.M., Meckler, A.N., Plessen, B., Robinson, R.S., Rosenthal, Y., Haug, G.H., 2009. Foraminiferal isotope evidence of reduced nitrogen fixation in the ice age Atlantic Ocean. Science 323, 244–248.
Sáez, A.G., Lozano, E., 2005. Body doubles. Nature 433, 111.
Sáez, A.G., Probert, I., Geisen, M., Quinn, P., Young, J.R., Medlin, L.K., 2003. Pseudo-cryptic speciation in coccolithophores. Proc. Natl. Acad. Sci. U. S. A. 100 (12), 7163–7168.
Schmitz, B., Pujalte, V., 2003. Sea-level, humidity, and land-erosion records across the initial Eocene thermal maximum from a continental-marine transect in northern Spain. Geology 31 (8), 689–692.
Schmitz, B., Pujalte, V., 2007. Abrupt increase in seasonal extreme precipitation at the Paleocene-Eocene boundary. Geology 35 (3), 215–218.
Schmitz, B., Pujalte, V., Molina, E., Monechi, S., Orue-Etxrbarria, X., Speijer, R.P., Alegret, L., Apellaniz, E., Arenillas, I., Aubry, M.-P., Baceta, J.-I., Berggren, W.A., Bernaola, G., Caballero, F., Clemmensen, A., Dinarès-Turell, J., Dupuis, C., Heilmann-Clausen, C., Orús, A.H., Knox, R., Martín-Rubio, M., Ortiz, S., Payros, A., Petrizzo, M.R., von Salis, K., Sprong, J., Steurbaut, E., Thomsen, E., 2011. The global Stratotype sections and points for the bases of the Selandian (Middle Paleocene) and Thanetian (Upper Paleocene) stages at Zumaia, Spain. Episodes 34 (4), 220–243.
Sigman, D.M., Altabet, M.A., McCorkle, D.C., Francois, R., Fischer, G., 2000. The $\delta^{15}N$ of nitrate in the Southern Ocean: nitrogen cycling and circulation in the ocean interior. J. Geophys. Res. Oceans 105 (C8), 19599–19614.
Speijer, R.P., 2003. Danian-Selandian sea-level change and biotic excursion on the southern Tethyan margin (Egypt). Geol. Soc. Am. Spec. Pap. 369, 275–290.
Steinmetz, J.C., Stradner, H., 1984. Cenozoic calcareous nannofossils from Deep Sea drilling Project Leg 75, southeast Atlantic Ocean. In: Hay, W.W., Sibuet, J.C. (Eds.), Initial Reports of the Deep Sea Drilling Project. 75(2). U.S. Government Printing Office, Washington, D.C., pp. 671–753.
Steurbaut, E., Sztrákos, K., 2008. Danian/Selandian boundary criteria and North Sea basin-Tethys correlations based on calcareous nannofossil and foraminiferal trends in SW France. Mar. Micropaleontol. 67 (1), 1–29.
Stradner, H., 1960. Über nannoplankton-invasionen im Sarmat des Wiener Beckens. Erdoël-Zeitschrift 76, 430–432.
Stradner, H., 1973. Catalogue of calcareous nannoplankton from sediments of Neogene Age in the eastern North Atlantic and Mediterranean Sea. In: Ryan, W.B.F., Hsü, K.J. (Eds.), Initial Reports of the Deep Sea Drilling Project. 13(2). U.S. Government Printing Office, Washington, D.C., pp. 1137–1199.
Stradner, H., Fuchs, R., 1980. Über nannoplanktonvorkommen im Sarmatien (Ober-Miozan) der centralen Paratethys in Niederösterreich und im Burgenland. Beitr. Paläontol. Österr. 7, 251–279.
Strauss, H., Peters-Kotig, W., 2003. The Paleozoic to Mesozoic carbon cycle revisited: the carbon isotopic composition of terrestrial organic matter. Geochem. Geophys. Geosyst. 4 (10), 1–15.
Švábenická, L., 1999. *Braarudosphaera*-rich sediments in the Turonian of the Bohemian Cretaceous Basin, Czech Republic. Cretac. Res. 20, 773–782.
Takano, Y., Hagino, K., Tanaka, Y., Horiguchi, T., Okada, H., 2006. Phylogenetic affinities of an enigmatic nannoplankton, *Braarudosphaera bigelowii* based on the SSU rDNA sequences. Mar. Micropaleontol. 60, 145–156.
Tesdal, J.E., Galbraith, E.D., Kienast, M., 2013. Nitrogen isotopes in bulk marine sediment: linking seafloor observations with subseafloor records. Biogeosciences 10 (1), 101–118.
de Vargas, C., Sáez, A.G., Medlin, L.K., Thierstein, H.R., 2004. Super-species in the calcareous plankton. In: Thierstein, H.R., Young, J.R. (Eds.), Coccolithophores: From Molecular Processes to Global Impact. Springer Verlag, pp. 271–298.
Varol, O., 1989. Palaeocene calcareous nannofossil biostratigraphy. In: Crux, J.A., van Heck, S.E. (Eds.), Nannofossils and their Applications. British Micropalaeontological Society 12. pp. 267–310.
Wada, E., Hattori, A., 1991. Nitrogen in the Sea: Forms, Abundances & Rate Processes. CRC Press, Florida, U.S.A. (208 pp).
Westerhold, T., Röhl, U., Raffi, I., Fornaciari, E., Monechi, S., Reale, V., Bowles, J., Evans, H.F., 2008. Astronomical calibration of the Paleocene time. Palaeogeogr. Palaeoclimatol. Palaeoecol. 257 (4), 377–403.
Westerhold, T., Röhl, U., Donner, B., McCarren, H.K., Zachos, J.C., 2011. A complete high-resolution Paleocene benthic stable isotope record for the central Pacific (ODP site 1209). Paleoceanography 26 (2), PA2216.
Young, J., 1990. Size variation of Neogene *Reticulofenestra* coccoliths from Indian Ocean DSDP cores. J. Micropalaeontol. 9 (1), 71–85.